February 2014

Thesis for Master Degree

Purification and Preliminary Crystal Structure Study of L-arabinose Isomerase from Thermophilic *Alicyclobacillus acidoalcarius* and *Geobacillus kaustophilus* HTA426

Graduate School of Chosun University

Department of Bio-Materials

Cao Thinh Phat

2014 년 2 월

석사학위논문

고온세균인 *Alicyclobacillus acidoalcarius* 및 *Geobacillus kaustophilus* **HTA426** 으로부터 **L-arabinose** 이성질화 효소의 분리 및 예비 결정 구조 연구

조선대학교 대학원

생물신소재학과

Cao Thinh Phat

고온세균인 *Alicyclobacillus acidoalcarius* 및 *Geobacillus kaustophilus* **HTA426** 으로부터 **L-arabinose** 이성질화 효소의 분리 및 예비 결정 구조 연구

Purification and Preliminary Crystal Structure Study of L-arabinose Isomerase from Thermophilic *Alicyclobacillus acidoalcarius* and *Geobacillus kaustophilus* HTA42

조선대학교 대학원

생물신소재학과

Cao Thinh Phat

고온세균인 *Alicyclobacillus acidoalcarius* 및 *Geobacillus kaustophilus* **HTA426** 으로부터 **L-arabinose** 이성질화 효소의 분리 및 예비 결정 구조 연구

지도교수 이성행

이 논문을 이학석사학위 신청 논문으로 제출함

2013 년 10 월

조선대학교 대학원

생물신소재학과

Cao Thinh Phat

Cao Thinh Phat 의 석사학위
논문을 인준함

위원장　조선대학교　조교수　송 희 상　(인)

위 원　조선대학교　부교수　방 일 수　(인)

위 원　조선대학교　부교수　이 성 행　(인)

2013 년 **11** 월

조선대학교 대학원

Purification and Preliminary Crystal Structure Study of L-arabinose Isomerase from Thermophilic *Alicyclobacillus acidoalcarius* and *Geobacillus kaustophilus* HTA426

This thesis is submitted to Graduate School of Chosun University in partial fulfilment of the requirements for the degree of Master of Science.

by

Cao Thinh Phat

Department of Bio-Materials, Graduate School,

Chosun University, Gwangju, Republic of Korea

2013.11

Approved by

Prof. Song Hee Sang, PhD _____

Prof. Bang Il Su, PhD _____

Major Advisor

Prof. Lee Sung Haeng, PhD _____

CONTENT

List of Figures iii

List of Tables iv

ABBREVIATIONS v

ABSTRACT vi

국문 초록 viii

Chapter 1: Introduction ..... - 1 -

Chapter 2: Materials and Methods ..... - 10 -

2.1. Materials ..... - 10 -

2.1.1. The pET-15b vector (Novagen®, Merck Millipore, Germany) ..... - 10 -

2.1.2. The vector constructs of AAAI and GKAI ..... - 10 -

2.1.3. The competant *E. coli* BL21 (DE3) cell strain ..... - 12 -

2.2. Transformation and Cell Culture of AAAI and GKAI ..... - 13 -

2.3. Purification of AAAI and GKAI ..... - 14 -

2.3.1. Preliminary purifying ..... - 14 -

2.3.2. Binding to Ni-NTA Agarose columns and eluting ..... - 14 -

2.3.3. Releasing N-terminal 6xHis-tagged ..... - 15 -

2.3.4. Gel filtrating ..... - 15 -

2.4. Crystallization of AAAI and GKAI ..... - 16 -

2.4.1. Hanging drop vapour diffusion method ..... - 16 -

2.4.2. Crystallization of AAAI and GKAI ..... - 17 -

2.5. Diffraction of AAAI and GKAI ..... - 18 -

Chapter 3: Results and Discussion ..... - 19 -

3.1. Expression and Purification of AAAI and GKAI ..... - 19 -

3.2. Crystallization and Data Collection of AAAI and GKAI ..... - 27 -

3.2.1. Crystallization and Data Collection of AAAI ..... - 27 -

3.2.2. Crystallization and Data Collection of GKAI ..... - 35 -

Chapter 4: Conclusion ..... - 42 -

Chapter 5: References ..... - 44 -

APPENDIX ..... - 48 -

ACKNOWLEDGEMENT ..... - 54 -

List of Figures

Figure 1.1: Part of the pentose phosphate pathway---------- - 2 -

Figure 1.2: The catalytic activity of L-arabinose isomerase (EC 5.3.1.4)---------- - 3 -

Figure 1.3: ECAI monomer and its structural homolog ECFI---------- - 7 -

Figure 2.1: The pET-15b vector map from Novagen®, Merck Millipore, Germany -------- 11 -

Figure 2.1: Process of vapour diffusion. ---------- 16 -

Figure 3.1: SDS-PAGE analysis of purified 6xHis-tagged AAAI (a) and intact AAAI (b) - 21 -

Figure 3.2: SDS-PAGE analysis of purified 6xHis-tagged GKAI (a) and intact GKAI (b) - 22 -

Figure 3.3: The size exclusion profile of AAAI ---------- 23 -

Figure 3.4: SDS-PAGE analysis of AAAI size exclusion profile---------- 24 -

Figure 3.5: The size exclusion profile of GKAI ---------- 25 -

Figure 3.6: SDS-PAGE analysis of GKAI size exclusion profile---------- 26 -

Figure 3.5: The initial forming crystals of AAAI---------- 29 -

Figure 3.6: The initial forming crystals of AAAI---------- 30 -

Figure 3.7: Crystals of AAAI ---------- 31 -

Figure 3.8: Crystals of AAAI ---------- 32 -

Figure 3.9: An X-ray diffraction image of AAAI---------- 33 -

Figure 3.10: Crystals of GKAI---------- 37 -

Figure 3.11: Crystals of GKAI---------- 38 -

Figure 3.12: Crystals of GKAI---------- 39 -

Figure 3.13: An X-ray diffraction image of GKAI crystal---------- 40 -

List of Tables

Table 1. Comparison of some features of three competent cells ---------- 12 -

Table 2. Initial screening conditions which produced AAAI crystals ---------- 27 -

Table 3. Crystallographic Data collection Statistics for AAAI---------- 34 -

Table 4. Initial screening conditions which produced GKAI crystals ---------- 35 -

Table 5. Crystallographic Data collection Statistics for GKAI---------- 41 -

ABBREVIATIONS

AI	L-arabinose isomerase
AAAI	*Alicyclobacillus acidocaldarius* L-arabinose isomerase
GKAI	*Geobacillus kaustophilus* HTA426 L-arabinose isomerase
IPTG	Isopropyl β-D-1-thiogalactopyranoside
EDTA	Ethylenediamine tetraacetic acid
PMSF	Phenylmethylsulfonyl flouride
PEG	Polyethylene glycol

ABSTRACT

Purification and Preliminary Crystal Structure Study of L-arabinose Isomerase from Thermophilic *Alicyclobacillus acidoalcarius* and *Geobacillus kaustophilus* HTA426

Cao Thinh Phat

Advisor: Prof. Lee Sung Haeng

Department of Bio-Materials

Graduate School of Chosun University

L-arabinose isomerase (AI) (EC 5.3.1.4), encoded by *ara*A gene, is an intracellular enzyme in various microorganisms that catalyzes the isomerization of L-arabinose to L-ribulose *in vivo*, it can also catalyze to conversion of D-galactose to D-tagatose *in vitro* due to structural similarity of L-arabinose and D-galactose.

Tagatose is a rare natural sugar which can be used as an edible sweetener in foods and beverages, or as an additive in pharmaceutical and cosmetic formulas. Currently, tagatose is a new potential drug for treating type-2 diabetes and obesity. Several methods have been established to manufacture tagatose, amongst them, an interesting biological method is enzymatic process using AI.

The isomerization of D-galactose to D-tagatose requires high temperature, mesophilic AIs therefore are of limited application. Thermophiles and hyperthermophiles are

interesting strains, with the obviously higher ratio of tagatose production's yields were reported. *Geobacillus kaustophilus* HTA426 and *Alicyclobacillus acidocaldarius* are two of thermophilic strains which could be examined more about their AIs' crystal structure to establish the catalytic mechanism as well as the biotechnological interest.

In this study, the *ara*A gene which were cloned from *G. kaustophilus* HTA426 and *A. acidocaldarius* were expressed and purified using Ni-NTA Agarose. The AIs from these strains, which denominated GKAI and AAAI respectively, were then crystallized and preliminary analyzed by X-ray crystallography. Data collections demonstrated that asymetric unit of the GKAI crystal contained six molecules, with Matthew's coefficient 2.25 $Å^3$ Da^{-1} and solvent content 45.39%, whilst asymetric unit of AAAI crystal contained nine molecules, with Matthew's coefficient 2.33 $Å^3$ Da^{-1} and solvent content 47.13%. The three-dimensional structure determination of AAAI and GKAI are currently in progress by molecular replacement and model building.

국문 초록

고온세균인 *Alicyclobacillus acidoalcarius* 및*Geobacillus kaustophilus* HTA426으로부터 L-arabinose 이성질화 효소의 분리 및 예비 결정 구조 연구

Cao Thinh Phat

지도교수 : 이 성 행

조선대학교 일반대학원

생물신소재학과

다양한 미생물 내에서 존재하는 L-arabinose isomerase (AI) 는 생체내에서 L-arabinose 를 L-ribulose 로 이성질화를 촉매하는 세포내 효소이며 또한 생체외 에서는 구조적 유사성 때문에 D-galactose 를 D-tagatose 로의 전환을 촉매할 수 있다.

Tagatose 는 음식과 음료수내 식용향료로서 이용할 수 있는 드문 천연 당일뿐만 아니라 약제와 화장품제조의 첨가제로도 이용될 수 있다. 현재 tagatose 는 type-2 당뇨병과 비만 처방을 위한 강력한 약물이다.

tagatose 제조를 위해 확립된 몇몇 방법들 중에 가장 관심 있는 생물학적인 방법이 AI 를 사용하는 효소를 이용한 과정이다.

D-galactose 의 D-tagatose 로의 이성질화는 높은 온도를 필요로 하여 중온성세균의 AIs 는 이용에 한계가 있다. 그래서, 고온성과 초고온성 세균은 tagatose 높은 생산율이 보고되어 있기 때문에 관심 있는 균들이다. 이중에 *Geobacillus kaustophilus* HTA426 와 *Alicyclobacillus acidocaldarius* 은 고온성 세균이고 생물공학적 관심 뿐만 아니라 기전을 확립하기 위해 결정구조를 조사하였다.

이 연구에서 *G. kaustophilus* HTA426 와 *A. acidocaldarius* 으로부터 클론된 araA 유전인자 단백질을 발현시켰고 Ni-NTA agarose 를 이용하여 정제하였다. 이러한 균으로부터 AIs 는 각각 GKAI, AAAI 로 명명하고, 단백질을 x-ray crystallography 에 의해 결정화하고 예비 데이터를 얻었다. 데이터 수집 결과 GKAI 결정은 asymmetric unit 에 Matthew's coefficient 가 2.25 $Å^3$ Da^{-1} 이고 solvent content 가 45.39%와 함께 6 개를 포함한 반면, AAAI 결정은 Matthew's coefficient 2.33 $Å^3$ Da^{-1} and solvent content 47.13%과 함께 9 개를 포함하는 것으로 분석되었다. 현재는 AAAI 와 GKAI 의 3 차원구조 결정은 MR 과 model building 에 의해 진행 중이다.

Chapter 1: Introduction

L-arabinose isomerase (AI) (EC 5.3.1.4) belongs to the arabinose isomerase family. AI catalyzes the reversible isomerization of L-arabinose to L-ribulose *in vivo*, the first step of aldopentose metabolism (or pentose phosphate pathway) (Figure 1.1) in bacteria which involved arabinose operon to utilize arabinose as a carbon source (Izumori *et al.*, 1978, Cheetham & Wootton, 1993, Manjasetty & Chance, 2006, Kim *et al.*, 2002). Arabinose operon of *Escherichia coli* has been thoroughly investigated up to now, several strains have also been studied and compared. It was demonstrated that there might be a few differences in arabinose operon components amongst various strains, but in concision, it includes some genes: *ara*A, *ara*B, *ara*C and *ara*D, *ara*E, *ara*F, *ara*G, *ara*H…, therein *ara*C is regulatory gene and *ara*A code for L-arabinose isomerase (James W. Patrick, 1968, Sá-Nogueira & Lencastre, 1989, Schleif, 2010, 2000).

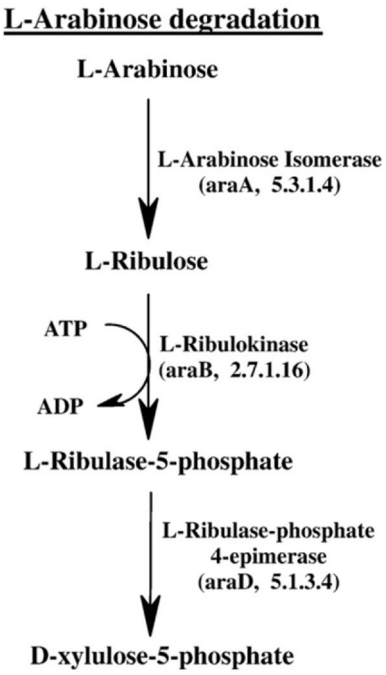

Figure 1.1: Part of the pentose phosphate pathway

The conversion of L-arabinose into D-xylulose-5-phosphate is shown.

AI is also able to catalyze the conversion of D-galactose to D-tagatose *in vitro* (Figure 1.2) due to the structural similarity which were explained by Cheetham and Wootton (1993): the sharing of hydroxyl group at C_3-C_4 in a *cis*-configuration relative to each other (Cheetham *et al.*, 1993, F. Jorgensen, 2004).

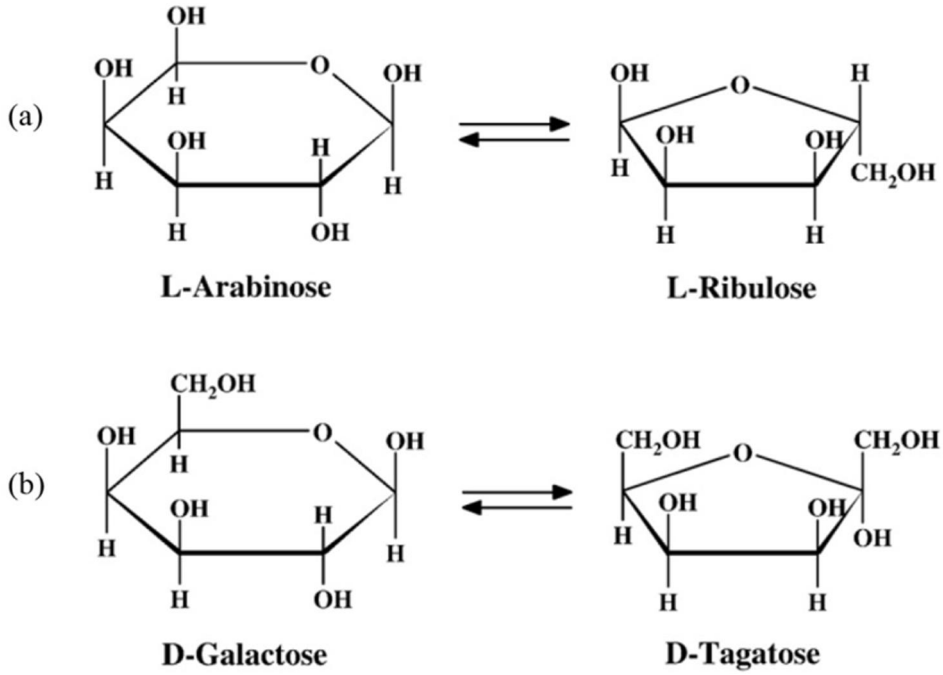

Figure 1.2: The catalytic activity of L-arabinose isomerase (EC 5.3.1.4)

(a) The first intracellular step in the catabolism of L-arabinose by E. coli is catalyzed by the enzyme L-arabinose isomerase *in vivo*.

(b) The bioconversion of D-galactose into D-tagatose *in vitro* by L-arabinose isomerase. L-arabinose and D-galactose share the L-*cis*-hydroxyl configuration at C3 and C4, therefore D-galactose could be a substrate of L-arabinose isomerase for producing D-tagatose (Cheetham *et al.*, 1993, Jorgensen *et al.*, 2004).

D-tagatose,a stereoisomer of D-fructose, is a rare ketohexose which has been considered as an attractive commercial sugar due to its benefits. First, tagatose is a low calorie (nonfattening) and full-bulk natural sweetener. It is 92% as sweet as sucrose when tested in 10% aqueous solutions, hence tagatose is virtually indistinguishable in taste from sucrose, but

the caloric value of tagatose is 1.5 kcal/g whilst sucrose is 40 kcal/g. Second, the safety of tagatose has been investigated. It was proved that tagatose gives no cooling effect, aftertaste or potentiation off-flavors, as well as no cariogenicity. Also no toxic effect and laxative effect of tagatose have been found. Therefore tagatose is a potential substituted sweetener. Since 2001, tagatose has been attained GRAS (Generally Recognized As Safe) status under U.S. Food and Drug Administration (FDA) regulations, and approved for use in foods and beverages in USA, EU, Australia, New Zealand, Korea, Japan, Brasil… Further studies demonstrated that tagatose causes no increase glucose levels in blood according to physiological examinations therefore giving safe for type 2 diabetic patients, and more benefits of tagatose such as anti-aging, anti-anemic, anti-hemopilia…have been reported, implicated that tagatose could be also use as an additive in pharmaceutical and cosmetic formulas. (Levin *et al.*, 1995, Levin, 2002, Cheetham *et al.*, 1993, Roh *et al.*, 2000, Manjasetty *et al.*, 2006, Kim *et al.*, 2002, Wanarska & Kur, 2012)

Tagatose occurs naturally in various foods such as sterilized and powdered cow's milk, ultra-high-temperature milk, hot cocoa, a variety of cheeses, yogurt, dairy products and other natural sources such as *Sterculia setigera* (tropical date tree) gum exudate, *Roccella hypomecha*, *Roccella linearis*, *Roccella fucoformis* (lichens)…, however, the amounts are too small for economic recovery (Levin *et al.*, 1995). Methods to manufacture tagatose have been establishing so far. For instances, isomerizing galactose derived from lactose hydrolysisusing calcium catalyst at relatively low temperature, then neutralizing the intermediate complex to yield tagatose (Beadle *et al.*, 1992), disadvantages of this chemical method are by-product and chemical waste formation, and enegy-consuming to cool the reaction mixture. Biological methods were studied and applied, such as oxidation of galacitol using microorganisms such as *Mycobacterium smegmatis* (Izumori & Tsuzaki, 1988), *Arthrobacter globiformis* (Izumori

et al., 1984), *Enterobacter agglomerans* (Muniruzzaman *et al.*, 1994)…, however, galacitol is more expensive than galactose therefore not available as a raw material for commercial application (Roh *et al.*, 2000, Wanarska *et al.*, 2012). Besides, bioconversion of psicose, a rare sugar, is a method using various strains of *Mucoraceae* fungi (Yoshihara *et al.*, 2006), but an inconvenience of this process is psicose producing step from fructose.

Another biological approach is enzymatic process, using L-arabinose isomerase, a microorganism intracellular enzyme. In fact, recent studies demonstrated that this process has conveniences of cost and manipulation as well as enviromental safety. Due to interesting benefits of tagatose, studies on AIs, especially in molecular level, should be brought about thoroughly.

Microorganisms which could be used as sources for isolating AI have been reported, therein, mesophiles such as *Escherichia coli* (Yoon *et al.*, 2003), *Bacillus halodurans* (Lee, Choe, et al., 2005b), *Lactobacillus plantarum* (Chouayekh *et al.*, 2007), *Lactobacillus fermentum* (Xu et al., 2011); thermophiles such as *Geobacillus stereothermophilus* (Lee, Choe*, et al.*, 2005b), *Geobacillus thermodenitrificans* (Kim & Oh, 2005), *Anoxybacillus flavithermus* (Li et al., 2011), *Bacillus stereothermophilus* US100 (Rhimi & Bejar, 2006), *Bacillus stereothermophilus* IAM11001 (Cheng, Mu & Jiang, 2010), *Alicyclobacillus acidocaldarius* (Lee, Lee, et al., 2005), *Thermus* sp. IM6501 (Kim *et al.*, 2003), *Acidothermus cellulolytic* (Cheng, Mu, Zhang*, et al.*, 2010), *Thermoanaerobacter mathranii* (Jorgensen *et al.*, 2004); and hyperthermophiles such as *Thermotoga neapolitana* (Kim *et al.*, 2002) and *Thermotoga maritima* (Wanarska *et al.*, 2012, Lee *et al.*, 2004).

Actually, there are differences in catalytic activity of AIs from mesophiles, thermophiles and hyperthermophiles, and thermostability of them may concern in tagatose

production (Manjasetty *et al.*, 2006, Lee, Hong, *et al.*, 2005, Lee, Choe, *et al.*, 2005a, Wanarska *et al.*, 2012). To clarify these differences, it is necessary to study the structural crystal of AIs, and in addition, the responsibility of divalent metal ion like Mn^{2+} in catalytic activity as well as in stability of AIs should be elucidated. As consequence, the first AI crystal structure described in molecular level is from *Escherichia coli* (ECAI) (Manjasetty *et al.*, 2006) (Fig.1.1). Previously, biophysical and electron microscopy studies predicted native ECAI exists as hexamer form both in crystals and in solutions (Patrick & Lee, 1969, Wallace *et al.*, 1978, Pauley *et al.*, 1972), whilst thermophilic AIs exists as tetramer in solution (Lee *et al.*, 2004). The comparison of structure and sequence alignment of several AIs showed the conservation of residues in the subunit interactions, amongst mesophilic, thermophilic and hyperthermophilic enzymes (Manjasetty *et al.*, 2006). This report then suggested the posibility of putative active site architecture. Other studies also revealed the contribution of Mn^{2+} in intrinsic activity and thermostability of ECAI, and suggested the modification in hexamer forming related to manganous ion (James W. Patrick, 1971).

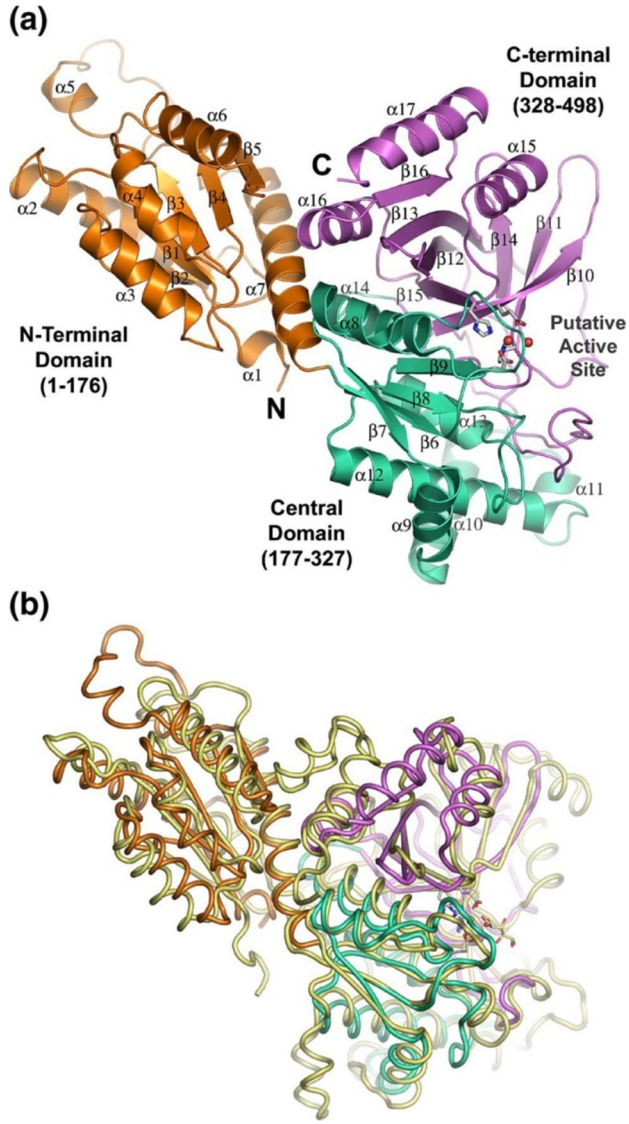

Figure 1.3: ECAI monomer and its structural homolog ECFI

(a) Ribbon diagram of ECAI monomer coloured by domains. The secondary structure elements, domains, N termini and C termini are labelled. A stick view of the putative active site is also depicted. (b) Superposition of the Cα trace of monomers: subunit of ECAI isomerase coloured by domains and ECFI (PDB ID, 1FUI) shown in yellow. (Manjasetty *et al.*, 2006)

The tagatose conversion of mesophilic ECAI is 34% at 308 K (Roh *et al.*, 2000). However, according to kinetic studies, the tagatose production ratio seems to be higher and reaction rates will increase at higher temperature, thus thermostable AIs are interesting to industrial applications (Manjasetty *et al.*, 2006, Lee *et al.*, 2004, Kim *et al.*, 2002, Lee, Hong, *et al.*, 2005, Lee, Choe, *et al.*, 2005a). In another aspect, the investigation of AI activity of ECAI indicated that Mn^{2+} contributes very slightly to the enzyme stablity and absolutely not requires for the catalytic activity (James W. Patrick, 1971, Manjasetty *et al.*, 2006). Kinetic study of another mesophilic AI, from *Bacillus halodurans* (BHAI), showed that the catalysis does not depend on Mn^{2+} presence (Lee, Choe, *et al.*, 2005a). In contrast, divalent metal ions appear to be an absolute requirement for catalytic activity of thermophilic AIs, furthermore, these types of AIs are more stable in the presence of Mn^{2+} (Lee, Choe, *et al.*, 2005a). For instance, hyperthermophile *Thermotoga neapolitana* AI (TNAI) has been reported that the conversion increased following the raising of incubation temperature, precisely, the maximum activity of the L-arabinose isomerization and D-galactose isomerization is at 358 K in the presence of divalent metal ion (Co^{2+} or Mn^{2+}), and the yield of tagatose conversion of 68% at 353 K (Kim *et al.*, 2002). Another hyperthermophilic AI, *Thermotoga maritima* (TMAI), which has 94.8% identical amino acids of TNAI, showed the similar characteristic of thermostable, especially in the presence of Co^{2+}/Mn^{2+}, and the yield of tagatose conversion of 56% at 353 K (Lee *et al.*, 2004). It is necessary to investigate more about structure of thermophilic AIs to clarify the catalytic activity as well as the contribution of divalent metal ions in the stability of enzymes.

Alicyclobacillus acidocaldarius, former name is *Bacillus acidocaldarius*, is an thermoacidophilic bacterium which were isolated by Darland and Brock (1971), from acid thermal environments, both aqueous and terrestrial, at temperature from 318 K up to 343 K

(optimally 333 K to 338 K) and at pH values from 2.0 to 6.0 (optimally 3 to 4) (Darland & Brock, 1971, Wisotzkey *et al.*, 1992). It was reclassified onto *Alicyclobacillus* genus by Wisotzkey et. al. (1992) through comparative 16S rRNA sequence analysis (Wisotzkey *et al.*, 1992). The AI from *Alicyclobacillus acidocaldarius*, which denominated AAAI, has 497 amino acids, molecular weight of monomer is 56.043 kDa, theoretical pI value is 5.51 and calculated extinction coefficient value (ε) is 1.448. The sequential alignment of AAAI shares 61% identity of ECAI (Appendix 1).

Geobacillus kaustophilus HTA426, former name is *Bacillus kaustophilus*, is a thermophilic strain which can grow at limit temperature up to 347 K (optimally 333 K) (Takami *et al.*, 2004). It was isolated from the deepest sea mud of Mariana Trench by Takami et. al. (1996), and reclassified onto *Geobacillus* genus by Nazina et. al. (2001) through comparative analysis of 16S rRNA sequences and fatty acid compositions (Takami *et al.*, 2004, Takami *et al.*, 1997, Nazina *et al.*, 2001). The AI from *G. kaustophilus* HTA426, which denominated GKAI, has 497 amino acids, molecular weight of monomer is 56.2 kDa, theoretical pI value is 5.42 and calculated extinction coefficient value (ε) is 1.541. The sequential alignment of GKAI shares 61% identity of ECAI (Appendix 1) and 96% identity of AAAI (Appendix 3).

Those types of AI above might be potential sources for tagatose production. Thus, their crystal structure and biochemical characteristics should be examined.

In attempt to clarify the structure of thermophilic AIs, as well as their characteristics concerning tagatose production, in this study, AAAI and GKAI were overexpressed, purified, then crystallized and diffracted by X-ray.

Chapter 2: Materials and Methods

2.1. Materials

2.1.1. The pET-15b vector (Novagen®, Merck Millipore, Germany)

The pET System is developed by Novagen® (Merck Milipore, Germany) for the cloning and expression of recombinant proteins in *E. coli*. Target genes are cloned in pET plasmids under control of strong bacteriophage T7 transcription and optionally translation signals; expression is induced by providing a source of T7 RNA polymerase in the host cell (pET System Manual 11th, 2003).

pET-15b vector carries an N-terminal His-Tag® sequence followed by a thrombin site and three cloning site. The sequence is numbered by the pBR322 convention, so the T7 expression region is reversed on the circular map. The cloning/expression region of the coding strand transcribed by T7 RNA polymerase is shown in Fig. 2.1.

2.1.2. The vector constructs of AAAI and GKAI

The *ara*A genes from *Alicyclobacillus acidocaldarius* and *Geobacillus kaustophilus* HTA426 were cloned into pET15b expression vector, the construct names are pET15b-AAAI and pET15b-GKAI, respectively. These plasmids were obtained from Department of Applied Biosciences, Kyungpook National University, Daegu 702-701, South Korea.

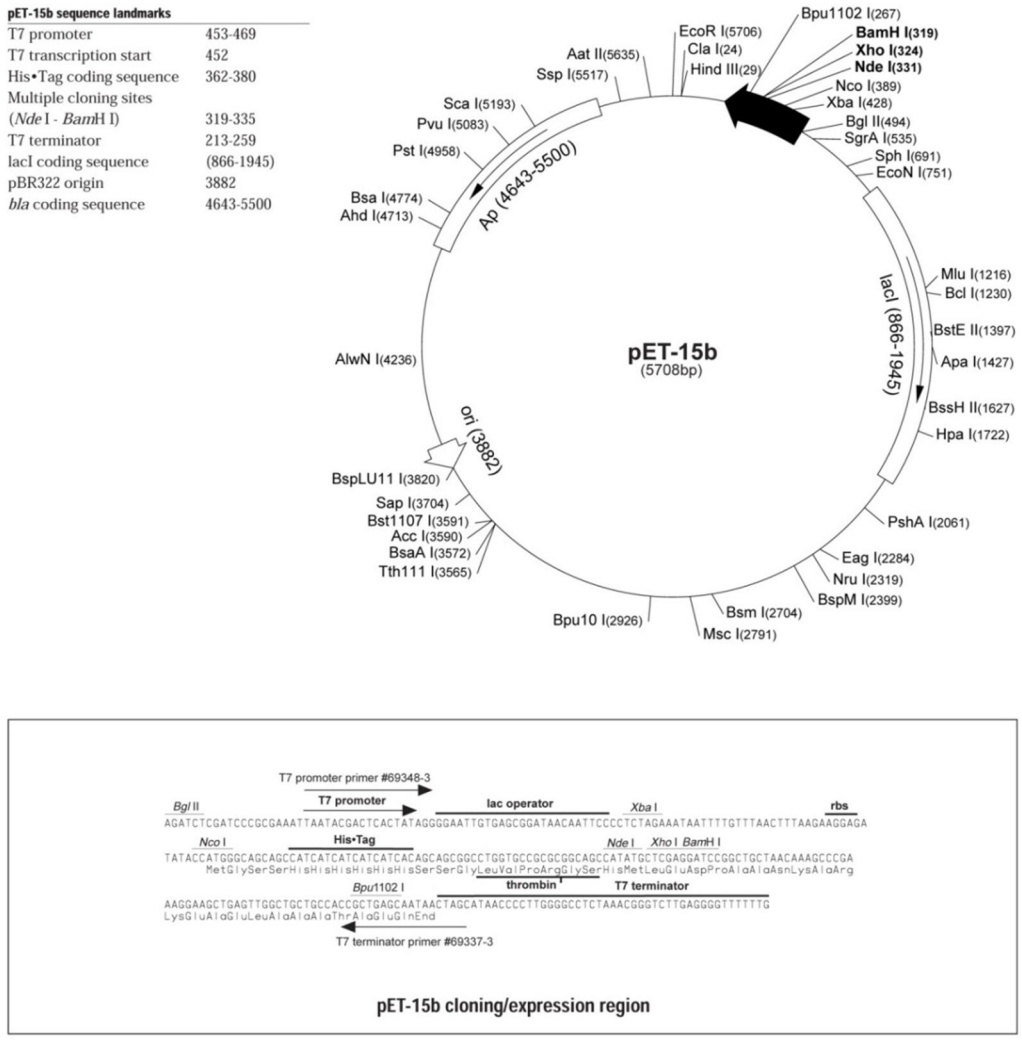

Figure 2.1: The pET-15b vector map from Novagen®, Merck Millipore, Germany

2.1.3. The competant *E. coli* BL21 (DE3) cell strain

E. coli BL21 (DE3) is one of the protein expression host strains using the T7 promoter. As the *E. coli* B strains, this strain lacks both the *lon* protease and the *ompT* outer membrane protease, which can degrade proteins during purification (Grodberg & Dunn, 1988). The genotype of BL21 (DE3) strain is: F^- ompT gal dcm lon $hsdS_B(r_B^- m_B^-)$ λ(DE3 [lacI lacUV5-T7 gene 1 ind1 sam7 nin5]) (OpenWetWare). The (DE3) designation indicates that the host is a lysogen of λ prophage (DE3), and therefore carries a chromosomal copy of the T7 RNA polymerase gene under control of the lacUV5 promoter (inducible by addition of IPTG or using an auto-inducible medium). Table 2.1 compares the features of some strains including BL21 (DE3).

Table 1. Comparison of some features of three competent cells

(from www.genomics.agilent.com)

Expression strain	Induction Method	Advantages	Disadvantages
BL21(DE3) competent cells	Isopropyl-1-thio-β-D-galactopyranoside (IPTG) induction of T7 polymerase from lacUV5 promoter	High-level expression	Leaky expression of T7 polymerase can lead to uninduced expression of potentially toxic proteins
BL21(DE3)pLysS competent cells	Isopropyl-1-thio-β-D-galactopyranoside (IPTG) induction of T7 polymerase	Ease of induction	Slight inhibition of induced expression when compared with BL21(DE3)
BL21 competent cells	Infection with lambda bacteriophage CE6	Tightest control of uninduced expression	Induction not as efficient as DE3 derivatives
			Induction (infection) process more cumbersome

2.2. Transformation and Cell Culture of AAAI and GKAI

The pET15b-AAAI and pET15b-GKAI were transformed into *E. coli* BL21 strain using Heat Shock procedure: the tubes containing 50 μL of competent *E. coli* BL21 (DE3) cells stock from 193 K were thawed on ice for 5 minutes. 1 μL of each plasmid pET15b-AAAI/ pET15b-GKAI was inoculated into BL21 (DE3) cells and gently pipetted, then incubated on ice for 20 minutes. The tubes of cells with DNA were heated in waterbath at 315 K in 90 seconds and immediately put back on ice for 5 minutes. 1 mL of non-antibiotic Lubria Broth media was added into each tube, the tubes were then incubated in shaking incubator at 310 K with 200 rpm for 60 minutes.

After 60 minutes incubation, the tubes were centrifuged at 8,000 rpm for 3 minutes. 950 μL of supernatant was removed. 100 μL of remains were carefully mixed by pipetting and 20 μL of them were spread onto Luria Agar plates (Laboratorios Conda, Spain) containing 100 μg mL^{-1} ampicillin. These plates were then incubated at 310 K for 16 hours.

The cells which contained plasmids would survive under the effect of ampicillin. The colonies were picked up and grown in 3 litters of Luria Broth media (10 g/L tryptone, 5 g/L yeast extract and 10 g/L NaCl) containing 100 μg mL^{-1} ampicillin at 310 K on shaking incubator with 200 rpm. When the absorbance of culture fluid reached approximately 0.8 – 1.0 at 600 nm, cells were induced by 1 mM of isopropyl β-D-1-thiogalactopyranoside (IPTG) at 310 K. After 5 hours induction, cells were harvested by centrifuging 5,000*g* in 30 minutes.

2.3. Purification of AAAI and GKAI

2.3.1. Preliminary purifying

The pellet after harvesting were resuspended in Lysis Buffer (20 mM Tris-HCl pH 7.5, 500 mM NaCl and 10 mM imidazole) supplemented with 1 mM of phenylmethylsulfonyl fluoride (PMSF) as an proteinase inhibitor, and 1 mM of ethylenediaminetetraacetic acid (EDTA). The mixtures were then disrupted by sonicating. The time of sonicating is 4 minutes with amplification of 30%, pulse on 20 seconds and pulse off 20 seconds.

After sonicating, the lysates were centrifuged at 20,000*g* in 30 minutes to remove cell debris. The supernatants were collected and heated 333 K in waterbath in 10 minutes and centrifuged again. Due to thermostability trait of thermophilic AIs, some impure protein would be denaturated. In the presence of EDTA, divalent ion especially Mn^{2+} would be sequestrated and removed from the supernatant. The latter supernatants were collected and further purified using Ni-NTA Agarose columns.

2.3.2. Binding to Ni-NTA Agarose columns and eluting

Ni-NTA Agarose (Qiagen GmbH, Germany) is a nickel-nitrilotriacetic acid (Ni-NTA) metal-affinitiy chromatography matrix for purifying recombinant proteins which have been tagged with 6 consecutive histidine residues (6xHis-tagged).

3 mL of suspended Ni-NTA Agarose (in 20% ethanol) were packed into column for each type of AIs. These columns were equilibrated with 2 column volumes of Lysis Buffer. The supernatants after heating at 333 K were loaded onto these columns. By using pumping machine (Econo Pump, Bio-Rad, USA), the fluid stream was adjusted to 1 mL min^{-1} of speed. The columns were then washed by 5 column volumes of Washing Buffer (20 mM Tris-HCl

pH 7.5, 500 mM NaCl and 20 mM imidazole), the fluid stream was set in 2 mL min^{-1} of speed. After this step, the protein samples were eluted by Eluting Buffer (20 mM Tris-HCl pH 7.5, 500 mM NaCl and 250 mM imidazole).

All the collected samples above were loaded and run on 12% sodium dodecyl sulfate – polyacrylamide gel electrophoresis (SDS-PAGE), then visuallized by Coomassive Brilliant Blue.

2.3.3. Releasing N-terminal 6xHis-tagged

The elutions were dialyzed in Dialysis Buffer (20 mM Tris-HCl pH 7.5 and 150 mM NaCl) to decrease the high salt concentration (500 mM NaCl and 250 mM imidazole) in eluting step above. Dialyzing step was brought about overnight at room temperature.

The 1000 mM stock solution of calcium chloride was added into the protein solution to the final concentration of 2 mM. With 10 miligrams of protein, we used approximately 35 NIH units of human α-thrombin (Haematologic Technologies Inc., USA) to perform the cleaving His-tag out of the target protein. The cutting step was carried out 60 minutes at room temperature. After that, 1 mM of phenylmethylsulfonyl fluoride (PMSF) and 1 mM of ethylene diaminetetraacetic acid (EDTA) were added to inhibit the enzyme reaction.

2.3.4. Gel filtrating

Gel filtration chromatography, or size exclusion chromatography is a method in which molecules in solution are separated by their size. For this method, we used two products of GE Healthcare (USA): prepacked HiLoad™ 16/600 Superdex™ 200 prep grade column and ÄKTA FPLC™ Purifier System. The column was equilibrated by 20 mM Tris pH

7.5 and 50 mM NaCl, then the sample was injected into column by a 5 mL loop. The fluid stream speed was set in 1 mL min^{-1} and each collected fraction was 2 mL.

Fractions were examined by 12% sodium dodecyl sulfate – polyacrylamide gel electrophoresis (SDS-PAGE) and visualized by Coomassie Brilliant Blue.

2.4. Crystallization of AAAI and GKAI

2.4.1. Hanging drop vapour diffusion method

The hanging drop vapour diffusion technique is the most popular method for the crystallization of macromolecules. The principle of this technique is, a drop composed of a mixture of sample and reagent is placed in a vapour equilibration with a liquid reservoir of reagent, by the manner which is shown in Fig.2.1.

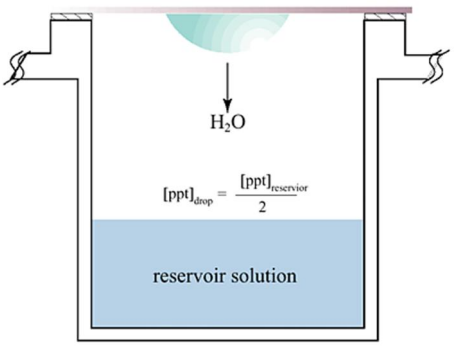

Figure 2.1: Process of vapour diffusion.

Typically the drop contains a lower reagent concentration than the reservoir. To achieve equilibrium, water vapour leaves the drop and eventually ends up in the reservoir. As water leaves the drop, the sample undergoes an increase in relative supersaturation. Both the

sample and reagent increase in concerntration as water leaves the drop for the reservoir. Equilibration is reached when the reagent concentration in the drop is approximately the same as that in the reservoir.

2.4.2. Crystallization of AAAI and GKAI

The purified AAAI and GKAI were concentrated to approximately 6 mg mL^{-}1 and 9 mg mL^{-}1 in 20 mM Tris-HCl pH 7.5 and 50 mM NaCl. Three fold of Mn^{2+} (which compares with protein concentration) was added to protein solution. Due to molecular weight of AAAI and GKAI are 56 kDa and 56.2 kDa, respectively, the amount of manganese chloride which could be supplemented are 320 μM for protein concentration of 6 mg mL^{-1} and 480 μM for protein concentration of 9 mg mL^{-1}.

Protein complexes with and without Mn^{2+} were performed crystallizing by hanging drop vapour diffusion technique. Therein, a drop was made by mixing 1.5 μL of protein sample with 1.5 μL of reservoir solution. For this method, 24 well plates were used and each reservoir volumn was 400 μL.

To find out the conditions which could bring the crystallization, we screened by commercial kits below:

- Hampton Research (USA) comprises of Index, SaltRx 1, SaltRx 2, Crystal Screen, Crystal Screen 2, Crystal Screen Lite, PEG/Ion Screen, PEG/Ion 2 Screen.

- Emerald Biosystems (USA) comprises of Wizard I, Wizard II, Wizard III, Wizard IV.

All conditions were placed in 293 K incubator, the time which the crystals appeared were recorded. After that, suitable conditions were improved for best crystallizing by creating the variety of pH range, precipitants and salt concentrations and screening again.

When suitable crystals were chosen, they would be soaked in the appropriate cryoprotectant solutions, and flash-cooled in liquid nitrogen for the X-ray diffraction. The cryoprotectant solutions were made by supplementing the amount of glycerol in order that the total concentration of the precipitant of reservoir solution (usually is polyethyleneglycol) and glycerol is approximately 20-35%

2.5. Diffraction of AAAI and GKAI

Crystals were mounted in stream of cold nitrogen (100 K). X-ray diffraction data were collected on beamline PAL-5C at Pohang Light Source (Pohang, Korea), using ADSC Quantum 315 CCD detector, oscillation of 1.0º and 5 s exposure per frame over a 360º range at a wavelength of 0.97951 Å. During diffraction, the cryoprotected crystals were kept in a cryogenic N_2-gas stream (~ 100 K) and diffracted finally to a maximum resolution of 2.70 Å. The diffraction data sets were indexed and scaled with program HKL-2000 (HKL Research Inc.) and diffraction statistics are shown in Table 1 and Table 2. The initial structure solution were determined by molecular replacement using the CCP4 program MOLREP and the structure of AI from *E. coli* (Manjasetty et al., 2006) as a search model. Model building and refinement are being carried out with the program COOT (Emsley & Cowtan, 2004) and the program PHENIX (Adams *et al.*, 2002).

Chapter 3: Results and Discussion

3.1. Expression and Purification of AAAI and GKAI

We firstly examined the induction of the transformed BL21 (DE3) cells according to the concentrations of IPTG and the temperature of induction. We set the IPTG concentrations are 0.5 mM and 1 mM, the induction temperature are 310 K (for 5 hours) and 291 K (for overnight). The results (data not shown) demonstrated that the IPTG concentration of 1 mM are better for the induction, regardless of the temperature. However, in the step of releasing 6xHis-tagged by thrombin, it was failed in case of GKAI. The reason has still not cleared, however, it might be predicted that there was an incorrect folding during the expression of GKAI under the effect of low temperature (291 K) overnight. Therefore, we chose the induction condition of both AAAI and GKAI transformed cells is: 1 mM IPTG at 310 K for 5 hours.

After eluting by high concentration of imidazole, a significant amount of His-AAAI and His-GKAI were successfully obtained as soluble form with expected molecular weight of ~58 kDa including N-terminal extra residues (6xHis-tagged) and thrombin cleavage site, although more than 80% of expressed proteins presented in inclusion body (Figure 3.1a and Figure 3.2a, lanes 3 to 5), indicating that most AAAIs and GKAIs expressed in *E. coli* are not properly folded during expression. However, AAAIs and GKAIs in soluble fractions (Figure 3.1a and Figure 3.2a, lane 5) might keep their stable conformations as existed at high temperature by following observations. First, after heating treatment at 333 K for 20 minutes, most AAAIs and GKAIs remained without any significant denaturation (Figure 3.1a and Figure 3.2a, lane 5 and lane 6). Second, AAAIs and GKAIs completely bound to Ni-NTA

Agarose column (Figure 3.1a and Figure 3.2a, lane 7 and lane 8), then be eluted with high concentration of imidazole as were the case of other thermophilic and hyperthermophilic AIs (Lee, Hong, *et al.*, 2005, Hong *et al.*, 2011a). Third, the entailed extra residues harbouring 6xHis and protease cleavage site at N-terminus was successfully removed to generate intact AAAI (56 kDa) and GKAI (56.2 kDa) (Figure 3.1b and Figure 3.2b), suggesting that the protease cleavage sites of these cases are appropriately exposed to thrombin through correct folding. These observations, however, were not enough to demonstrate the recombinant AAAI and GKAI preserved their original active conformation without any significant unfolding at elevated temperature. The isomerization activity examination of these AIs should be brought about in further studies to confirm this aspect.

The results as shown in figure 3.1b and figure 3.2b demonstrated there was a thin band remained in soluble fractions of both AAAI and GKAI, with approximately 40 kDa of molecular weight, after thrombin cutting step. We then tried to performed anion exchanging using MonoQ™ 5/50 GL column (GE Healthcare, USA), but it was not successfully removed by this method (data not shown). Once again, the protein samples were injected to HiLoad™ 16/600 Superdex™ 200 prep grade column (GE Healthcare, USA) for size exclusion chromatography. The protein samples were separated into 2 peaks (Figure 3.3 and Figue 3.5). Fractions were then examined by 12% SDS-PAGE, this band had still trivially remained, indicated that the purity of protein samples are more than 98% and worthwhile to crystallization trials.

After size exclusion method, fractions which were equivalent to peak 2 were collected and performed crystallization screening.

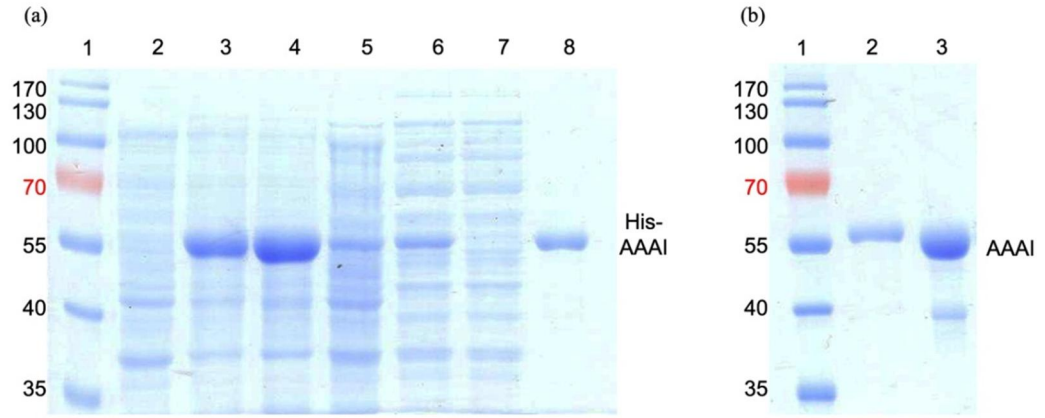

Figure 3.1: SDS-PAGE analysis of purified 6xHis-tagged AAAI (a) and intact AAAI (b)

(a) The bacterial lysate and purified recombinant fusion proteins were analysed using 12% SDS-PAGE. Lane 1, molecular weight ladder (kDa). Lane 2, lysate from uninduced cells. Lane 3, lysate from induced cells. Lane 4, pellet from induced cells. Lane 5, supernatant (soluble fraction) from induced cells. Lane 6,supernatant after heat treatment at 333 K for 20 mins. Lane 7, unbound fractions for the Ni-NTA agarose column. Lane 8, purified6xHis-tagged AAAI.

(b) The extra 17 amino acids including 6xHis-tagged were removed by thrombin digestion. Lane 1, molecular weight ladder (kDa). Lane 2, 6xHis-tagged AAAI (~58kDa). Lane 3, thrombin digested AAAI (~56kDa).

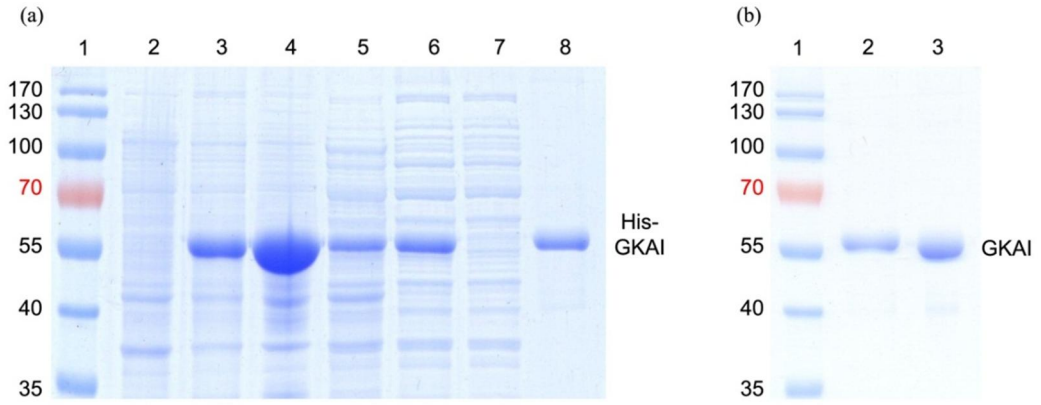

Figure 3.2: SDS-PAGE analysis of purified 6xHis-tagged GKAI (a) and intact GKAI (b)

(a) The bacterial lysate and purified recombinant fusion proteins were analysed using 12% SDS-PAGE. Lane 1, molecular weight ladder (kDa). Lane 2, lysate from uninduced cells. Lane 3, lysate from induced cells. Lane 4, pellet from induced cells. Lane 5, supernatant (soluble fraction) from induced cells. Lane 6, supernatant after heat treatment at 333 K for 20 mins. Lane 7, unbound fractions for the Ni-NTA agarose column. Lane 8, purified 6xHis-tagged GKAI.

(b) The extra 17 amino acids including 6xHis-tagged were removed by thrombin digestion. Lane 1, molecular weight ladder (kDa). Lane 2, 6xHis-tagged GKAI (~58kDa). Lane 3, thrombin digested GKAI (~56kDa).

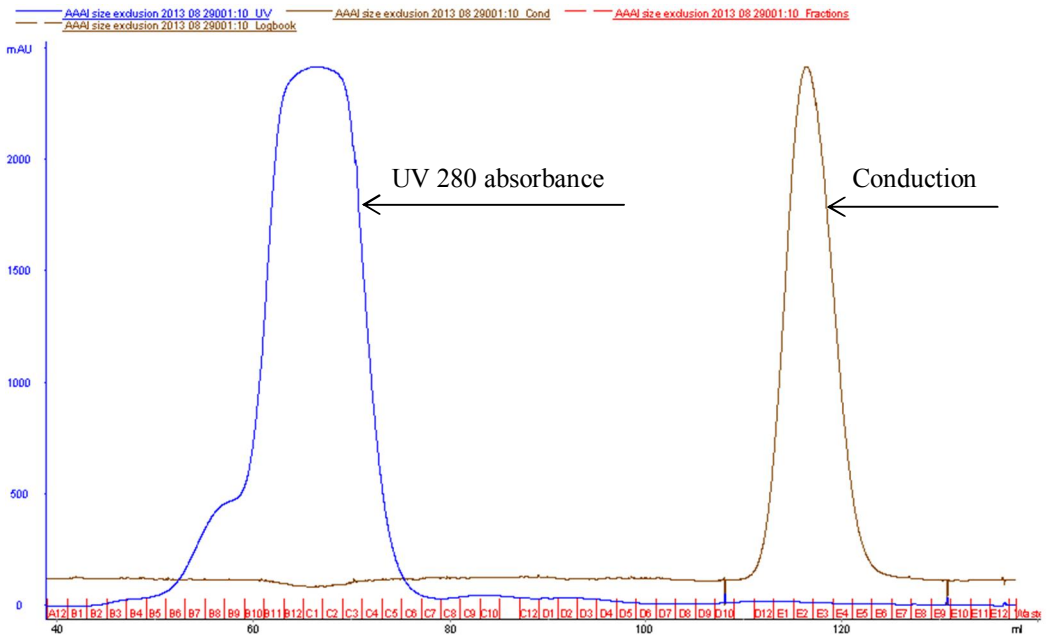

Figure 3.3: The size exclusion profile of AAAI

The size exclusion profile of AAAI performing by ÄKTA FPLC™ Purifier System, using HiLoad™ 16/600 Superdex™ 200 prep grade column. The protein sample was separated into 2 peaks. Fractions were examined by 12% SDS-PAGE and fractions from B10 to C5 (equivalent to peak 2) were collected and performed crystallization.

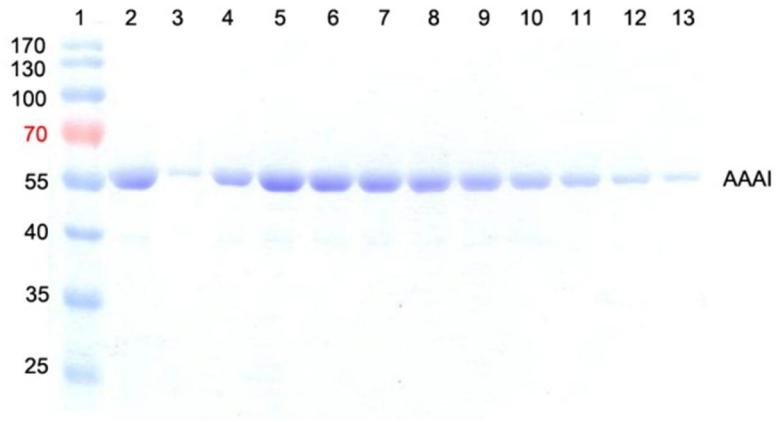

Figure 3.4: SDS-PAGE analysis of AAAI size exclusion profile

The purity of AAAI after size exclusion method was analyzed by 12% SDS-PAGE. Lane 1, molecular weight ladder (kDa). Lanes from number 2 to number 13 stand for fractions from B6 to C5, respectively, which are shown in Figure 3.3. There is no difference between peak 1 (fractions B6 to B9) and peak 2 (fractions B10 to C5), however, only fractions which are corresponding to peak 2 were collected to crystallization trials.

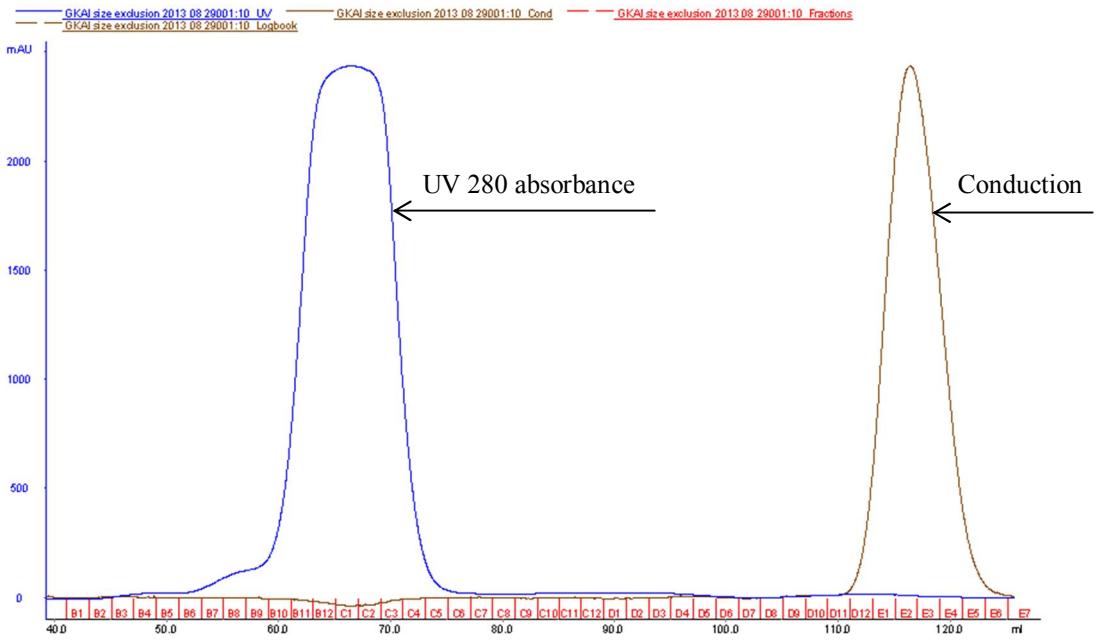

Figure 3.5: The size exclusion profile of GKAI

The size exclusion profile of GKAI performing by ÄKTA FPLC™ Purifier System, using HiLoad™ 16/600 Superdex™ 200 prep grade column. The protein sample was separated into 2 peaks. Fractions were examined by 12% SDS-PAGE and fractions from B11 to C4 (equivalent to peak 2) were collected and performed crystallization.

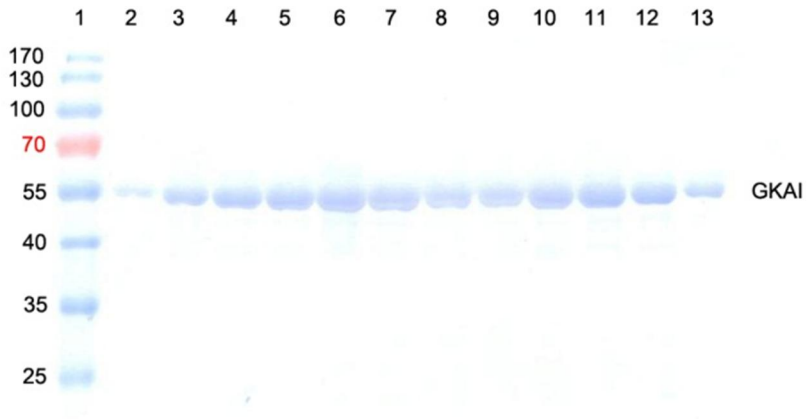

Figure 3.6: SDS-PAGE analysis of GKAI size exclusion profile

The purity of GKAI after size exclusion method was analyzed by 12% SDS-PAGE. Lane 1, molecular weight ladder (kDa). Lanes from number 2 to number 13 stand for fractions from B6 to C5, respectively, which are shown in Figure 3.5. There is no difference between peak 1 (fractions B7 to B10) and peak 2 (fractions B11 to C4), however, only fractions which are corresponding to peak 2 were collected to crystallization trials.

3.2. Crystallization and Data Collection of AAAI and GKAI

3.2.1. Crystallization and Data Collection of AAAI

In fact, AAAI was difficult to form the crystal. It took a quite long time (five days to more than one week) to a few of AAAI crystals appear between much of precipitate (Fig.3.1, Fig.3.2, Fig.3.3, Fig.3.4). Amongst screening reagent kits above, we obtained three major conditions that produced AAAI crystals, shown in Table 2 below:

Table 2. Initial screening conditions which produced AAAI crystals

Condition	Buffer	Salt	Precipitant
Wizard I No.10 (Emerald Biosystems)	0.1 M Tris base – HCl pH 7.0		20% (w/v) PEG 2000 MME
Wizard II No. 39 (Emerald Biosystems)	0.1 M CAPS – NaOH pH 10.5	0.2 M sodium chloride	20% (w/v) PEG 8000
Wizard III No.8 (Emerald Biosystems)		0.2 M potassium nitrate	20% PEG 3350

Initially, both crystals were small, amorphous and aggregated into the clusters (Figure 3.1), or fragile thin blades (Figure 3.2), hence those were not appropriate to diffraction trials. We attempted to improved those conditions by making a variety of buffer pH range, salt concentration and precipitants concentration. Crystals appeared with more clear shapes: irregular cube, short rod-shape…but data collections had been still not successful. We improved further with Hampton Research Additive Screen™, in which, a drop was added 0.2 μL of one additive. There were two major conditions which produced good-looking crystals:

- 20% PEG 3350, 0.2 M potassium nitrate adding 0.2 μL of 300 mM glycyl-glycyl-glycine

- 20% PEG 3350, 0.2 M potassium nitrateadding 0.2 μL of 20% (w/v) benzamidine HCl.

The second condition (which was added by benzamidine HCl) produced thin blade crystals, sometimes they emerged as hexagonal blades, and this kind of crystal had got the best diffraction data (Table 3). Once, we attempted to improve this condition by adding benzamidine HCl into the setting of a variety of the precipitant concentration (10 – 30% w/v of PEG 3350 and PEG 2000 MME) and salt concentration (100 – 400 mM of potassium nitrate).

In order to obtain an insight into the molecular and structural basis of such metal-dependent distinct properties with AAAI, we screened crystallization conditions for AAAI with and without Mn^{2+}. The crystallization condition consisting of 20 – 25% PEG 3350 and 200 mM potassium nitrate adding benzamidine HCl as an additive finally produced thin hexagonal blade crystals in the same drop regardless of the Mn^{2+} presence (Figure 3.3 and Figure 3.4). These crystals were successfully diffracted to 3.3 Å (Figure 3.5).

Based on the autoindexing and scaling using *HKL*-2000, the crystal belonged to space group P_3, with unit-cell parameters a = 152.939, b = 152.939, c = 173.547 Å and β = 90º (Table 3). A total of 270,631 reflections were measured in the resolution range of 50.0 – 3.3Å. An asymmetric unit is likely to contain nine AAAI molecules, which corresponded to a calculated Matthew's coefficient 2.33 $Å^3$ Da^{-1} and solvent content 47.13% (Matthews, 1968).

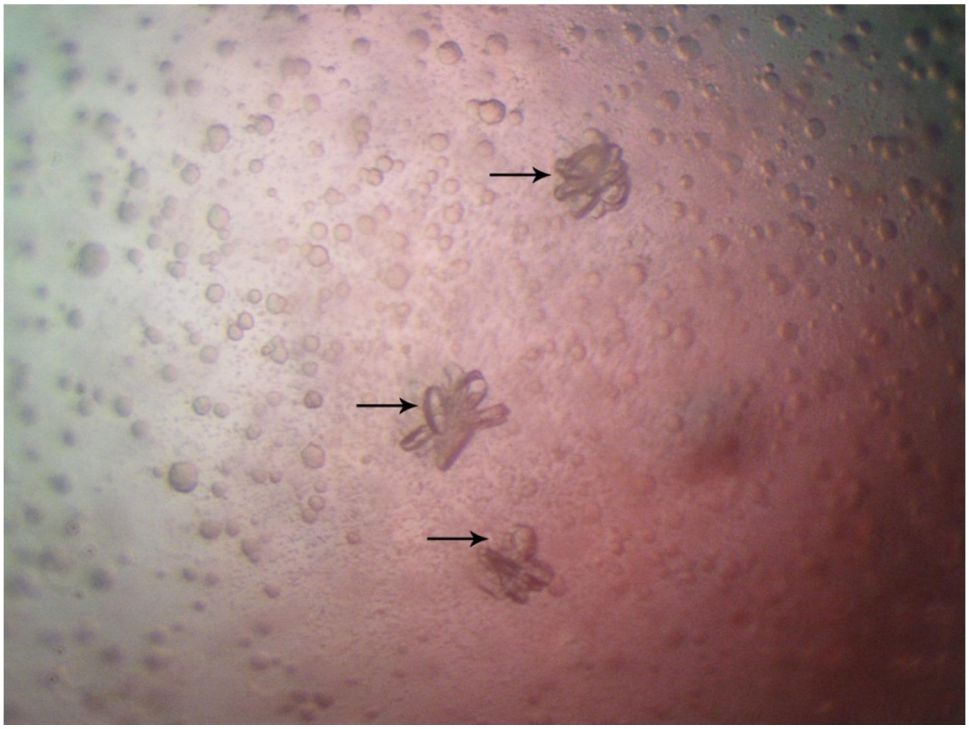

Figure 3.5: The initial forming crystals of AAAI

The initial crystals of AAAI were grown in 200 mM potassium nitrate and 20% (w/v) PEG 3350 (the arrow). These crystals formed the clusters and were small, therefore not suitable for X-ray diffraction.

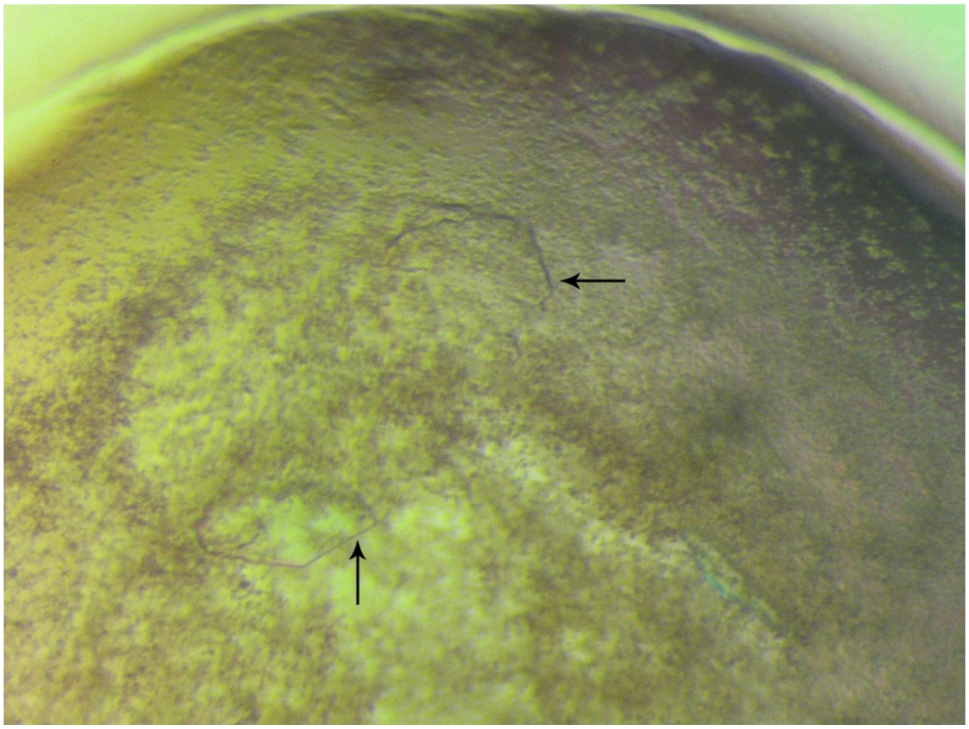

Figure 3.6: The initial forming crystals of AAAI

The initial crystals of AAAI were grown in 100 mM Tris-HCl pH 7.0 and 20% (w/v) PEG 2000 MME (the arrow). These crystaline shape appeared with thin blades. Much of precipitate formed. Diffraction data were not successfully obtained (data not shown).

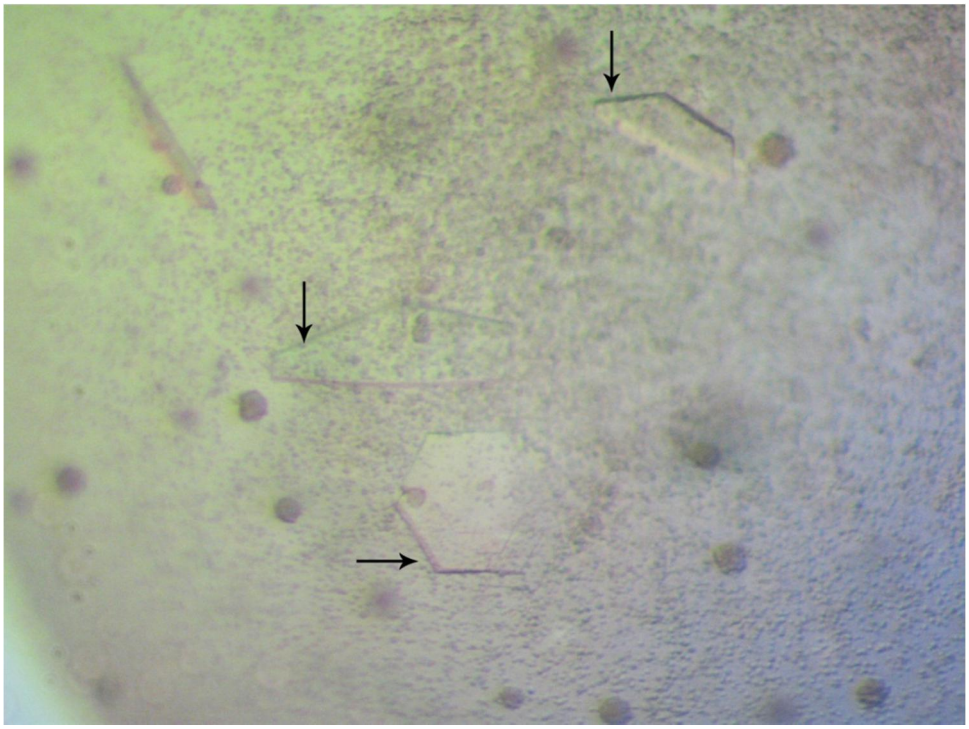

Figure 3.7: Crystals of AAAI

Crystal were grown in 200 mM potassium nitrate and 20% (w/v) PEG 3350 adding 0.2 μL of 20% (w/v) benzamidine HCl per drop. The crystaline shape appeared with thin blades. These crystals were stable in cryoprotectant containing 20% glycerol. Diffraction data were obtained by focusing the X-ray beam on the angles of the crystal (the arrow positions).

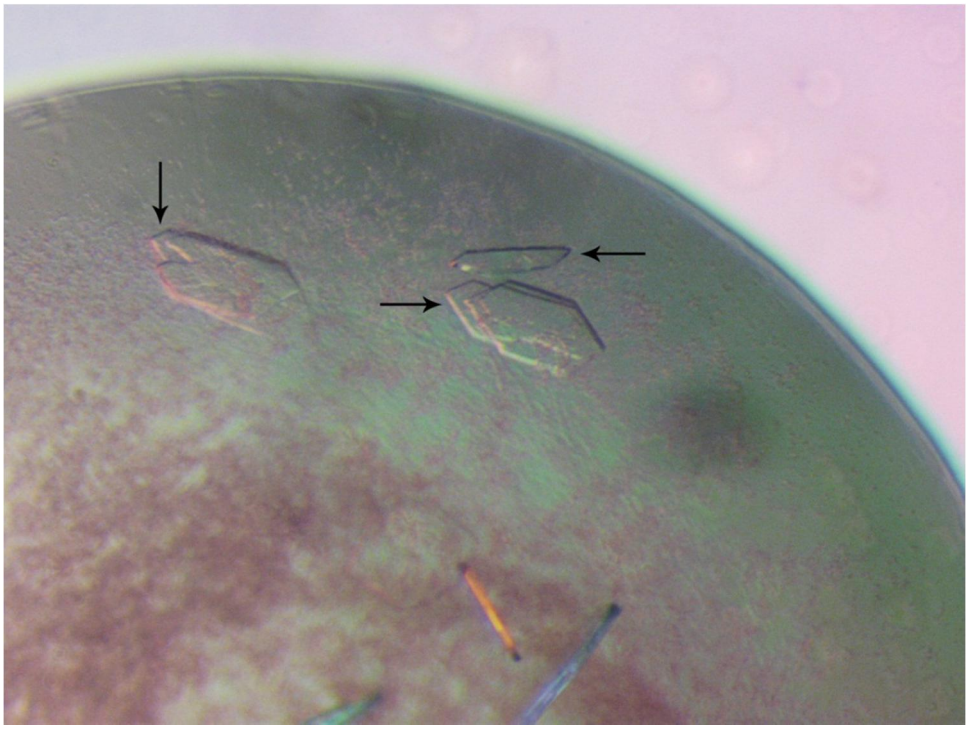

Figure 3.8: Crystals of AAAI

Crystal were grown in 200 mM potassium nitrate and 25% (w/v) PEG 3350 adding 0.2 μL of 20% (w/v) benzamidine HCl per drop. The crystaline shape appeared with thin blades. These crystals were stable in cryoprotectant containing 20% glycerol. Diffraction data were obtained by focusing the X-ray beam on the angles of the crystal (the arrow positions).

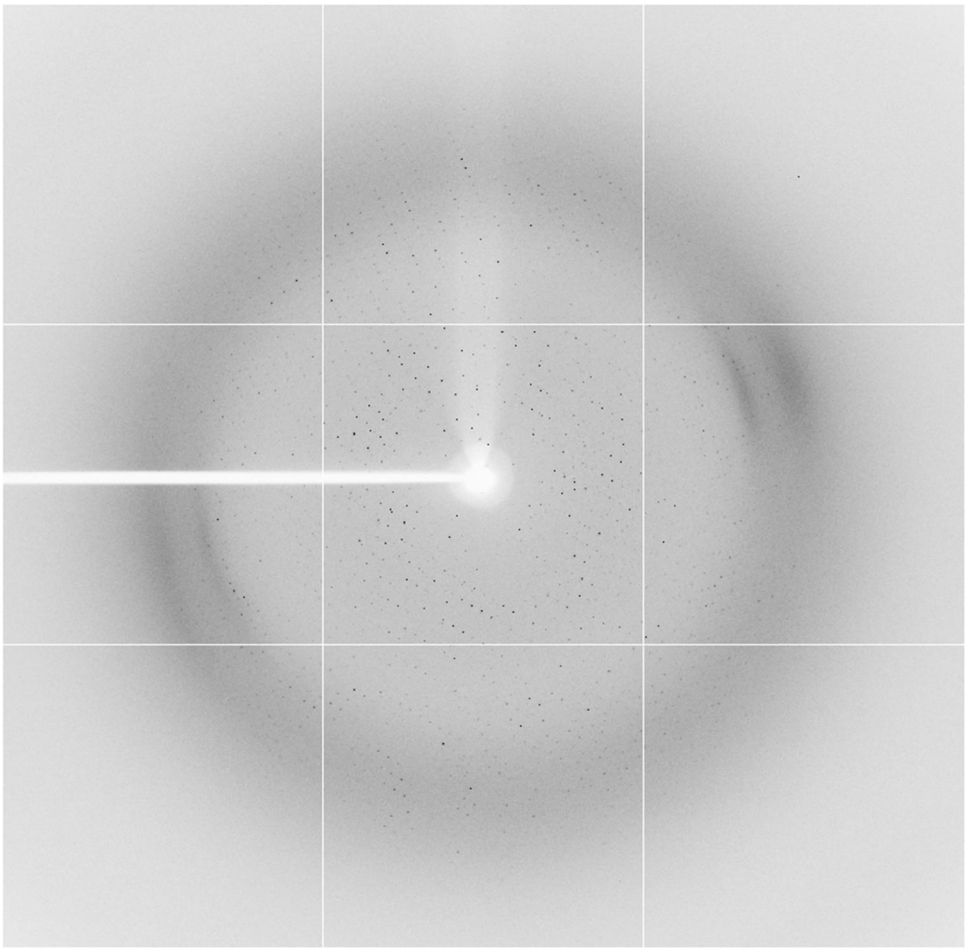

Figure 3.9: An X-ray diffraction image of AAAI

The diffraction data were collected from a single cryo-cooled AAAI crystal (from Fig 3.3), with a crystal-to-detector distance of 310 mm using a wavelength of 0.97951 Å. The oscillation was 1.0º per frame with 5 s exposure over a 320º range and the edge of the detector corresponds to 3.3 Å resolution.

Table 3. Crystallographic Data collection Statistics for AAAI

Diffraction statistics	
Beamline	PAL-5C
Wavelength (Å)	0.97950
Temperature (K)	100
Space group	*P*3
Cell parameters	
a, *b*, *c* (Å)	152.939, 152.939, 173.547
α, β, γ (°)	90.0, 90, 120
Data resolution (Å)	50.0 – 3.3 (3.36 – 3.30)
Completeness (%)	97.6 (97.3)
Redundancy	4.0 (3.8)
Total reflection	270631
Unique reflections	65295 (3088)
R-merge† (%)	13.3 (46.2)
Average I/σ	9.472 (2.65)
Matthew's coefficient ($Å^3$ Da^{-1})	2.33
Solvent content (%)	47.13
No. of molecules in the asymmetric unit	9

Values in parentheses correspond to highest resolution shell

†R-merge=$\Sigma(I-\langle I\rangle)/\Sigma I$; I and $\langle I\rangle$ are the intensity and the mean value of all the measurements of an individual reflection

3.2.2. Crystallization and Data Collection of GKAI

The GKAI crystals prompt formed after three to four days. Amongst screening reagent kits above, we obtained these major conditions that produced GKAI crystals, shown in Table 4 below:

Table 4. Initial screening conditions which produced GKAI crystals

Condition	Buffer	Salt	Precipitant
Index No.52 (Hampton Research)	0.1 M HEPES pH 7.5	0.2 M ammonium acetate	45% (v/v) 2-methyl-2,4-pentanediol
Crystal Screen Lite No.14 (Hampton Research)	0.1 M HEPES pH 7.5	0.2 M calcium chloride dihydrate	14% (v/v) PEG 400
Crystal Screen Lite No.23 (Hampton Research)	0.1 M HEPES pH 7.5	0.2 M magnesium chloride hexahydrate	15% (v/v) PEG 400
SaltRx 2 No.9 (Hampton Research)	1.8 M sodium phosphate monobasic, potassium phosphate dibasic pH 6.9		
Wizard I No.36 (Emerald Biosystems)	0.1 M imidazole pH 8.0	1 M sodium citrate	
Wizard II No.14 (Emerald Biosystems)	0.1 M potassium phosphate monobasic/ sodium phosphate dibasic pH 6.2	0.2 M sodium chloride	10% (w/v) PEG 1000

Initially, crystals from Wizard I No.36 condition were sufficient enough to use directly for diffraction tests (Figure 3.6). Although we attempted to improve the quality of the crystals further with a variety of salt concentrations and solution pH values from those

conditions above, also we screened with Hampton Research Additive Screen™, only crystals from original composition of Wizard I No.36 finally provided the best diffraction data (see Table 5).

In order to obtain an insight into the molecular and structural basis of such metal-dependent distinct properties with GKAI, we screened crystallization conditions for GKAI with and without Mn^{2+}. The crystallization condition consisting of 1 M sodium citrate, 0.1 M imidazole pH 8.0 finally produced long rod-shape and thin hexagonal blade in the same drop regardless of the Mn^{2+} presence (Figure 3.6). Of the two kinds of crystals, the rod-shaped crystal was diffracted to 2.7 Å (Figure 3.9).

Based on the autoindexing and scaling using *HKL*-2000, the crystal belonged to space group C_2, with unit-cell parameters a = 224.122, b = 152.952, c = 91.279 Å and β = 103.614º (Table 5). A total of 398,560 reflections were measured in the resolution range of 50.0 – 2.7 Å. An asymmetric unit is likely to contain six GKAI molecules, which corresponded to a calculated Matthew's coefficient 2.25 $Å^3$ Da^{-1} and solvent content 45.39% (Matthews, 1968).

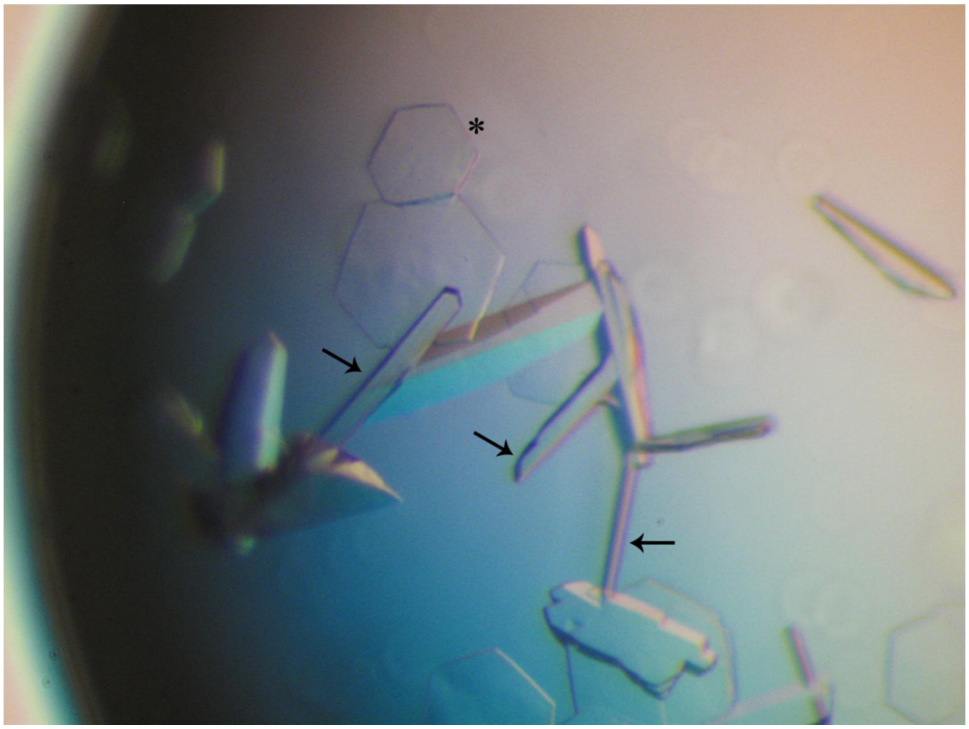

Figure 3.10: Crystals of GKAI

Crystals were grown in 1 M sodium citrate, 0.1 M imidazole pH 8.0 with 0.02 × 0.15 × 0.4 mm for rod-shaped crystals (arrows). Diffraction data were obtained only from the rod-shaped crystal, but those thin hexagonal crystals (asterisk) were poorly diffracted.

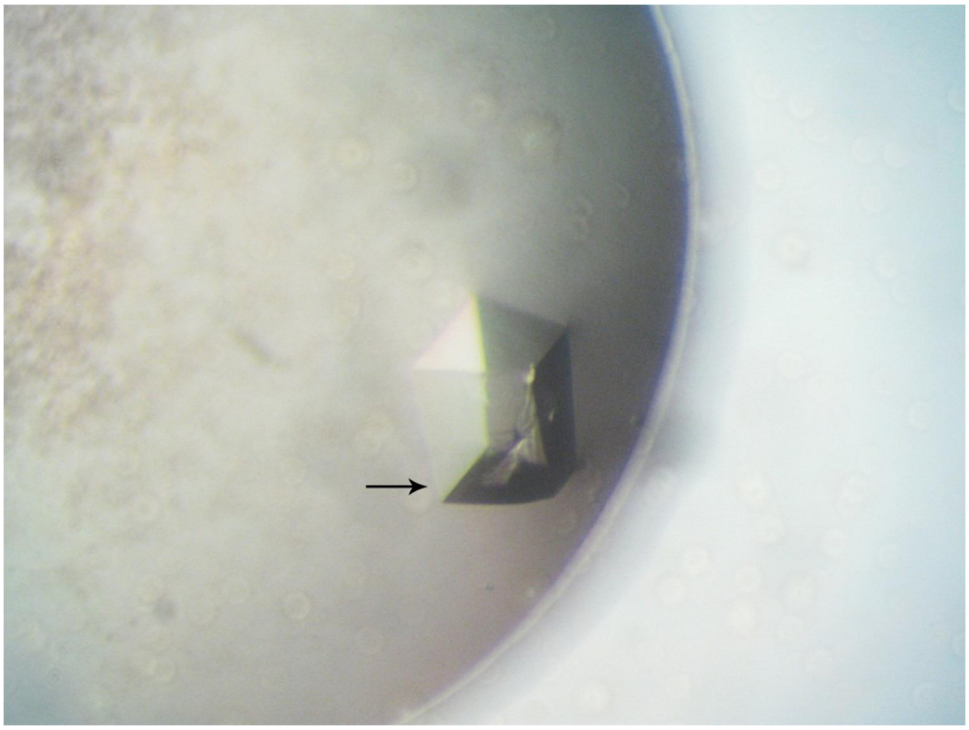

Figure 3.11: Crystals of GKAI

Crystals were grown in 1.8 M sodium sodium phosphate monobasic monohydrate/ potassium phosphate dibasic pH 5.0 adding 0.2 μL 40% (v/v) tert-butanol per drop. Only one polyhedron crystal formed in each drop. Diffraction data were obtained by focusing the X-ray beam on the angles of the crystal (arrow position) (data not shown).

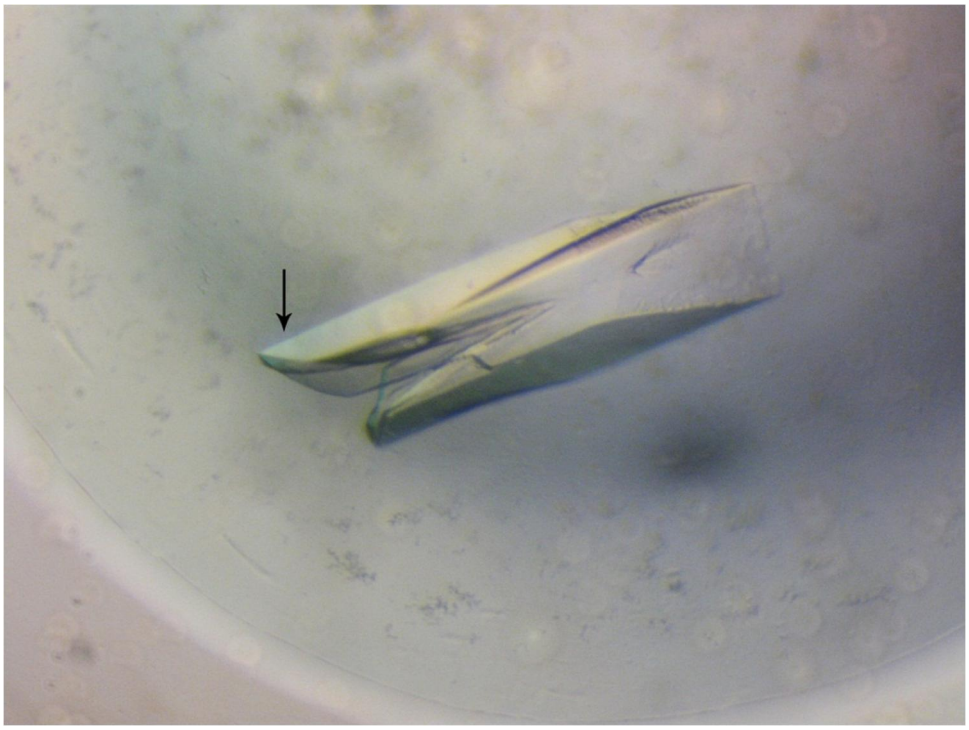

Figure 3.12: Crystals of GKAI

Crystals were grown in 2 M sodium sodium phosphate monobasic monohydrate/ potassium phosphate dibasic pH 6.8. Only one twin crystal formed in each drop. Diffraction data were obtained by focusing the X-ray beam on the end of the crystal (arrow position) (data not shown).

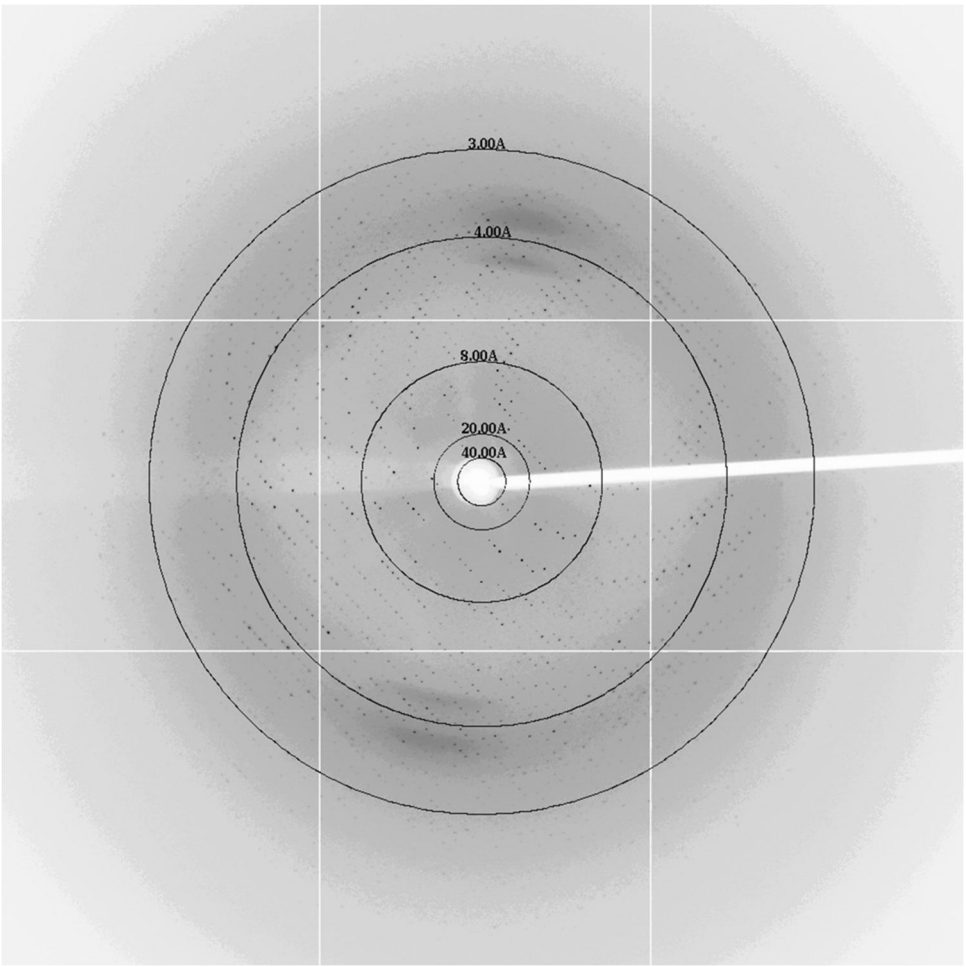

Figure 3.13: An X-ray diffraction image of GKAI crystal

The diffraction data were collected from a single cryo-cooled GKAI crystal with a crystal-to-detector distance of 310 mm using a wavelength of 0.97951 Å. The oscillation was 1.0º per frame with 5 s exposure over a 320º range and the edge of the detector corresponds to 2.7 Å resolution.

Table 5. Crystallographic Data collection Statistics for GKAI

Diffraction statistics	
Beamline	PAL-5C
Wavelength (Å)	0.97951
Temperature (K)	100
Space group	C_2
Cell parameters	
a, *b*, *c* (Å)	224.122, 152.952, 91.279
α, β, γ (°)	90.0, 103.614, 90.0
Data resolution (Å)	50.0 – 2.7 (2.75 – 2.7)
Completeness (%)	99.2 (99.9)
Redundancy	5.0 (5.0)
Total reflection	398560
Unique reflections	79807 (4031)
R-merge† (%)	9.6 (48.0)
Average I/σ	15.289 (2.992)
Matthew's coefficient ($Å^3$ Da^{-1})	2.25
Solvent content (%)	45.39
No. of molecules in the asymmetric unit	6

Values in parentheses correspond to highest resolution shell

†R-merge=$\Sigma(I-\langle I\rangle)/\Sigma I$; *I* and $\langle I\rangle$ are the intensity and the mean value of all the measurements of an individual reflection

Chapter 4: Conclusion

Although the amino acid sequences of mesophilic and thermophilic AIs are quite similar (>80%), their physicochemical properties are quite different (Hong *et al.*, 2011b). As described above, in contrast to mesophilic AIs that have little metal dependence on their activity, thermophilic AIs depend on divalent metal ions such as Mn^{2+} or Co^{2+} for their catalytic activity and thermostability. Previous reports proposed that such distinct properties between mesophilic and thermophilic AIs might be attributed to marginal contribution in a region-specific manner (Lee, Lee*, et al.*, 2005, Hong *et al.*, 2011b, Lee *et al.*, 2012).

In order to establish the contribution of divalent metal ion, particularly Mn^{2+}, in the biological conformation and catalytic activity of GKAI and AAAI, the crystallization screening in the presence of Mn^{2+} was also perfomed. Notably, the two different drops (+/-Mn^{2+}) produced their crystals in the same screening conditions, suggesting that endogenous Mn^{2+} might be incorporated into AAAI and GKAI during expression. In fact, we failed to get an apo enzyme even with EDTA treatments at 277 K. Therefore, if it is necessary to obtain apo forms for thermophilic AAAI and GKAI, metals bound the purified enzyme might have been depleted completely with EDTA at elevated temperatures (>333 K) as was done in (Lee, Choe*, et al.*, 2005c). If so then, it may provide information on the metal ion affinity of thermophilic AIs in comparison with mesophilic AIs.

Previously, the biophysical and electron microscopical studies demonstrated that native ECAI exists as a homo hexamer complex in solutions (Pauley *et al.*, 1972, Wallace *et al.*, 1978), while thermostable AIs exhibit majorly homotetramers as described in (Lee *et al.*, 2004, Jorgensen *et al.*, 2004, Manjasetty *et al.*, 2006). The crystal structure of AAAI and

GKAI therefore also needs to be thoroughly investigated to elucidate these differences as well as a metal dependent catalytic efficiency at elevated temperatures. For GKAI, the phases obtained by molecular replacement using *E. coli* AI as a search model, and converged to R-factor and R_{free} values of 21.8 % and 27.4 % from an initial round of refinement. For AAAI, the phases obtained by molecular replacement using GKAI as a search model, and converged to R-factor and R_{free} values of 25 % and 34 % from an initial round of refinement.

Further refinement is currently in progress to complete the quaternary structure of AAAI and GKAI.

Chapter 5: References

Adams, P. D., Grosse-Kunstleve, R. W., Hung, L. W., Ioerger, T. R., McCoy, A. J., Moriarty, N. W., Read, R. J., Sacchettini, J. C., Sauter, N. K. & Terwilliger, T. C. (2002). *Acta Crystallogr D Biol Crystallogr* **58**, 1948-1954.

Beadle, J. R., Saunders, J. P. & Thomas J. Wajda, J. (1992). Biospherics Incorporated, Beltsville, Md.

Cheetham, P. S. J. & Wootton, A. N. (1993). *Enzyme and Microbial Technology* **15**, 105-108.

Cheng, L., Mu, W. & Jiang, B. (2010). *Journal of the science of food and agriculture* **90**, 1327-1333.

Cheng, L., Mu, W., Zhang, T. & Jiang, B. (2010). *Appl Microbiol Biotechnol* **86**, 1089-1097.

Chouayekh, H., Bejar, W., Rhimi, M., Jelleli, K., Mseddi, M. & Bejar, S. (2007). *FEBS Letters* **227**, 260-267.

Darland, G. & Brock, T. D. (1971). *Journal of General Microbiology* **67**, 9-15.

Emsley, P. & Cowtan, K. (2004). *Acta Crystallogr D Biol Crystallogr* **60**, 2126-2132.

F. Jorgensen, O. C. H., P. Stougaard (2004). *Applied Microbiology and Biotechnology* **64**, 816-822.

Grodberg, J. & Dunn, J. J. (1988). *Journal of Bacteriology* **170**, 1245-1253.

Hong, Y.-H., Lee, D.-W., Pyun, Y.-R. & Lee, S. H. (2011a). *Journal of Agricultural and Food Chemistry* **59**, 12939-12947.

Hong, Y. H., Lee, D. W., Pyun, Y. R. & Lee, S. H. (2011b). *J Agric Food Chem* **59**, 12939-12947.

Izumori, K., Miyoshi, T., Tokuda, S. & Yamabe, K. (1984). *Applied and Enviromental Microbiology* **46**, 1055-1057.

Izumori, K. & Tsuzaki, K. (1988). *Journal of Fermentation Technology* **66**, 225-227.

Izumori, K., Ueda, Y. & Yamanaka, K. (1978). *Journal of Bacteriology* **133**, 413-414.

James W. Patrick, N. L. (1968). *The Journal of Biological Chemistry* **243**, 4312-4318.

James W. Patrick, N. L., Nora B. Barnes, Ellis Englesbergs (1971). *The Journal of Biological Chemistry* **246**, 5102-5106.

Jorgensen, F., Hansen, O. C. & Stougaard, P. (2004). *Appl Microbiol Biotechnol* **64**, 816-822.

Kim, B.-C., Lee, Y.-H., Lee, H.-S., Lee, D.-W., Choe, E.-A. & Pyun, Y.-R. (2002). *FEMS Microbiology Letters* **212**, 121-126.

Kim, H. J. & Oh, D. K. (2005). *Journal of biotechnology* **120**, 162-173.

Kim, J.-W., Kim, Y.-W., Roh, H.-J., Kim, H.-Y., Cha, J.-H., Park, K.-H. & Park, C.-S. (2003). *Biotechnology Letters* **25**, 963-967.

Lee, D.-W., Choe, E.-A., Kim, S.-B., Eom, S.-H., Hong, Y.-H., Lee, S.-J., Lee, H.-S., Lee, D.-Y. & Pyun, Y.-R. (2005a). *Archives of Biochemistry and Biophysics* **434**, 333-343.

Lee, D.-W., Hong, Y.-H., Choe, E.-A., Lee, S.-J., Kim, S.-B., Lee, H.-S., Oh, J.-W., Shin, H.-H. & Pyun, Y.-R. (2005). *FEBS Letters* **579**, 1261-1266.

Lee, D.-W., Jang, H.-J., Choe, E.-A., Kim, B.-C., Lee, S.-J., Kim, S.-B., Hong, Y.-H. & Pyun, Y.-R. (2004). 1397-1404.

Lee, D. W., Choe, E. A., Kim, S. B., Eom, S. H., Hong, Y. H., Lee, S. J., Lee, H. S., Lee, D. Y. & Pyun, Y. R. (2005b). *Arch Biochem Biophys* **434**, 333-343.

Lee, D. W., Choe, E. A., Kim, S. B., Eom, S. H., Hong, Y. H., Lee, S. J., Lee, H. S., Lee, D. Y. & Pyun, Y. R. (2005c). *Arch. Biochem. Biophys.* **434**, 333-343.

Lee, S. J., Lee, D. W., Choe, E. A., Hong, Y. H., Kim, S. B., Kim, B. C. & Pyun, Y. R. (2005). *Applied and environmental microbiology* **71**, 7888-7896.

Lee, S. J., Lee, Y. J., Kim, S. B., Kim, S. K. & Lee, D. W. (2012). *Appl Environ Microbiol* **78**, 8813-8816.

Levin, G. V. (2002). *Journal of Medicinal Food* **5**, 23-36.

Levin, G. V., Zehner, L. R., Saunders, J. P. & Beadle, J. R. (1995). *The American Journal of Clinical Nutrition* **62**, 1161-1168.

Li, Y., Zhu, Y., Liu, A. & Sun, Y. (2011). *Extremophiles : life under extreme conditions* **15**, 441-450.

Manjasetty, B. A. & Chance, M. R. (2006). *Journal of Molecular Biology* **360**, 297-309.

Matthews, B. W. (1968). *J Mol Biol* **33**, 491-497.

Muniruzzaman, S., Tokunaga, H. & Izumori, K. (1994). *Journal of Fermentation Technology* **78**, 145-148.

Nazina, T. N., Tourova, T. P., Poltaraus, A. B., Novikova, E. V., Grigoryan, A. A., Ivanova, A. E., Lysenko, A. M., Petrunyaka, V. V., Osipov, G. A., Belyaev, S. S. & Ivanov, M. V. (2001). *International Journal of Systematic and Evolutionary Microbiology* **51**, 433-446.

OpenWetWare E. coli genotypes: OpenWetWare.

Patrick, J. W. & Lee, N. (1969). *The Journal of Biological Chemistry* **244**, 4277-4283.

Pauley, J., Power, J. & Irr, J. (1972). *Journal of Bacteriology* **112**, 1247-1253.

pET System Manual 11th (2003). edited by M. Milipore, p. 4. Novagen.

Rhimi, M. & Bejar, S. (2006). *Biochimica et biophysica acta* **1760**, 191-199.

Roh, H. J., Kim, P., Park, Y. C. & Choi, J. H. (2000). *Biotechnology and Applied Biochemistry* **31**, 1-4.

Sá-Nogueira, I. & Lencastre, H. d. (1989). *Journal of Bacteriology* **171**, 4088-4091.

Schleif, R. (2000). *Trends in Genetics* **16**, 559-565.

Schleif, R. (2010). *FEMS Microbiology Review* **34**, 779-796.

Takami, H., Inoue, A., Fuji, F. & Horikoshi, K. (1997). *FEMS Microbiology Letters* **152**, 279-285.

Takami, H., Takaki, Y., Chee, G.-J., Nishi, S., Shimamura, S., Suzuki, H., Matsui, S. & Uchiyama, I. (2004). *Nucleic Acids Research* **32**, 6292-6303.

Wallace, L. J., Eiserling, F. A. & Wilcox, G. (1978). *The Journal of Biological Chemistry* **253**, 3717-3720.

Wanarska, M. & Kur, J. (2012). *Microbial Cell Factories* **11**.

Wisotzkey, J. D., Jr., P. J., Fox, G. E., Deinhard, G. & Poralla, K. (1992). *International Journal of Systematic Bacteriology* **42**, 263-269.

Xu, Z., Qing, Y., Li, S., Feng, X., Xu, H. & Ouyang, P. (2011). *Journal of Molecular Catalysis B: Enzymatic* **70**, 1-7.

Yoon, S.-H., Kim, P. & Oh, D.-K. (2003). *World Journal of Microbiology & Biotechnology* **19**, 47-51.

Yoshihara, K., Shinohara, Y., Hirotsu, T. & Izumori, K. (2006). *Journal of Bioscience and Bioengineering* **101**, 219-222.

APPENDIX

Appendix 1: Sequential alignment comparison of AAAI and ECAI

Sequence ID of ECAI: ref|WP_001596511.1| **Length:** 500

From http://www.ncbi.nlm.nih.gov/pubmed/

Score	Expect	Method	Identities	Positives	Gaps
639 bits(1649)	0.0	Compositional matrix adjust.	301/493(61%)	374/493(75%)	3/493(0%)

```
Query   8  YEFWFVTGSQHLYGEEALKQVEEHSMMIVNELNQDSVFPFPLVFKSVVTTPEEIRRVCLE  67
           YE WFV GSQHLYG E L+QV +H+  +VN LN ++  P  LV K + TTP+EI  +C +
Sbjct   7  YEVWFVIGSQHLYGPETLRQVTQHAEHVVNALNTEAKLPCKLVLKPLGTTPDEITAICRD  66

Query  68  ANASEQCAGVITWMHTFSPAKMWIGGLLELRKPLLHLHTQFNRDIPWDSIDMDFMNLNQS  127
           AN  ++CAG++ W+HTFSPAKMWI GL  L KPLL  HTQFN  +PWDSIDMDFMNLNQ+
Sbjct  67  ANYDDRCAGLVVWLHTFSPAKMWINGLTMLNKPLLQFHTQFNAALPWDSIDMDFMNLNQT  126

Query 128  AHGDREYGFIGARMGVARKVVVGHWEDPSVRERLAKWMRTAVAFAESRHLKVARFGDNMR  187
           AHG RE+GFIGARM     VV GHW+D  V ER+  WMR AV+  ++RHLKV RFGDNMR
Sbjct 127  AHGGREFGFIGARMRQQHAVVTGHWQDKQVHERIGSWMRQAVSKQDTRHLKVCRFGDNMR  186

Query 188  EVAVTEGDKVGAQIQFGWSVNGYGVGDLVQYIRDVSEQKINELLEEYAELYDIVPAGRQD  247
           EVAVT+GDKV AQI+FG+SVN + VGDLVQ +  +S+  +N L++EY   Y + PA +
Sbjct 187  EVAVTDGDKVAAQIKFGFSVNTWAVGDLVQVVNSISDGDVNALVDEYESCYTMTPATQIH  246

Query 248  GPVRESIREQARIELGLKAFLKDGNFAAFTTTFEDLHGMKQLPGLAVQRLMAEGYGFGGE  307
           G  R+++ E ARIELG+K FL+ G F AFTTTFEDLHG+KQLPGLAVQRLM +GYGF GE
Sbjct 247  GEKRQNVLEAARIELGMKRFLEQGGFHAFTTTFEDLHGLKQLPGLAVQRLMQQGYGFAGE  306

Query 308  GDWKTAALVRLMKVMADG--KGTSFMEDYTYHFEPGNEMILGAHMLEVCPTIAA-TRPRI  364
           GDWKTAAL+R+MKVM+ G   GTSFMEDYTYHFE GN+++LG+HMLEVCP+IAA  +P +
Sbjct 307  GDWKTAALLRIMKVMSTGLQGGTSFMEDYTYHFEKGNDLVLGSHMLEVCPSIAAEEKPIL  366

Query 365  EVHPLSIGGKEDPARLVFDGGEGAAVNASLIDLGHRFRLIVNEVDAVKPEHDMPKLPVAR  424
           +V  L IGGK+DPARL+F+   G A+ ASLIDLG R+RL+VN +D VK  H +PKLPVA
Sbjct 367  DVQHLGIGGKDDPARLIFNTQTGPAIVASLIDLGDRYRLLVNCIDTVKTPHSLPKLPVAN  426
```

```
Query 425  ILWKPRPSLRDSAEAWILAGGAHHTCFSFAVTTEQLQDFAEMAGIECVVINEHTSVSSFK  484
            LWK +P L  ++EAWILAGGAHHT FS A+    ++ FAEM  IE  VI+  T + +FK
Sbjct 427  ALWKAQPDLPTASEAWILAGGAHHTVFSHALNLNDMRQFAEMHDIEITVIDNDTRLPAFK  486

Query 485  NELRWNEVFWRGR  497
            + LRWNEV++  R
Sbjct 487  DALRWNEVYYGFR  499
```

Appendix 2: Sequential alignment comparison of GKAI and ECAI

Sequence ID of ECAI: ref|WP_001596511.1| **Length:** 500

From http://www.ncbi.nlm.nih.gov/pubmed/

Score	Expect	Method	Identities	Positives	Gaps
637 bits(1644)	0.0	Compositional matrix adjust.	301/493(61%)	374/493(75%)	3/493(0%)

```
Query   8   YEFWFVTGSQHLYGEEALKQVEEHSRIMVNEWNRDSVFPFPFVFKSVVTTPEEIRRVCLE  67
            YE WFV GSQHLYG E L+QV +H+  +VN  N ++  P   V K + TTP+EI  +C +
Sbjct   7   YEVWFVIGSQHLYGPETLRQVTQHAEHVVNALNTEAKLPCKLVLKPLGTTPDEITAICRD  66

Query  68   ANASEQCAGVVTWMHTFSPAKMWIGGLLELRKPLLHLHTQFNRDIPWDSIDMDFMNLNQS  127
            AN  ++CAG+V W+HTFSPAKMWI GL  L KPLL  HTQFN  +PWDSIDMDFMNLNQ+
Sbjct  67   ANYDDRCAGLVVWLHTFSPAKMWINGLTMLNKPLLQFHTQFNAALPWDSIDMDFMNLNQT  126

Query  128  AHGDREYGFIGARMGVARKVVVGHWEDPEVRERLAKWMRTAVAFAESRNLKVARFGDNMR  187
            AHG RE+GFIGARM     VV GHW+D +V ER+  WMR AV+  ++R+LKV RFGDNMR
Sbjct  127  AHGGREFGFIGARMRQQHAVVTGHWQDKQVHERIGSWMRQAVSKQDTRHLKVCRFGDNMR  186

Query  188  EVAVTEGDKVGAQIQFGWSVNGYGIGDLVQYIRDVSEQKVNELLDEYEELYDIVPAGRQE  247
            EVAVT+GDKV AQI+FG+SVN + +GDLVQ +  +S+  VN L+DEYE  Y + PA +
Sbjct  187  EVAVTDGDKVAAQIKFGFSVNTWAVGDLVQVVNSISDGDVNALVDEYESCYTMTPATQIH  246

Query  248  GPVRESIREQARIELGLKAFLQDGNFTAFTTTFEDLHGMKQLPGLAVQRLMAEGYGFGGE  307
            G  R+++ E ARIELG+K FL+ G F AFTTTFEDLHG+KQLPGLAVQRLM +GYGF GE
Sbjct  247  GEKRQNVLEAARIELGMKRFLEQGGFHAFTTTFEDLHGLKQLPGLAVQRLMQQGYGFAGE  306

Query  308  GDWKTAALVRLMKVMADG--KGTSFMEDYTYHFEPGNELILGAHMLEVCPTIAA-TRPRV  364
            GDWKTAAL+R+MKVM+ G   GTSFMEDYTYHFE GN+L+LG+HMLEVCP+IAA  +P +
Sbjct  307  GDWKTAALLRIMKVMSTGLQGGTSFMEDYTYHFEKGNDLVLGSHMLEVCPSIAAEEKPIL  366

Query  365  EVHPLSIGGKEDPARLVFDGGEGAAVNASLIDLGHRFRLIVNEVDAVKPEHDMPKLPVAR  424
            +V  L IGGK+DPARL+F+   G A+ ASLIDLG R+RL+VN +D VK  H +PKLPVA
Sbjct  367  DVQHLGIGGKDDPARLIFNTQTGPAIVASLIDLGDRYRLLVNCIDTVKTPHSLPKLPVAN  426
```

```
Query  425 ILWKPRPSLRDSAEAWILAGGAHHTCFSFAVTTEQLQDFAEMAGIECVVINEHTSVSSFK  484
            LWK +P L  ++EAWILAGGAHHT FS A+    ++ FAEM  IE  VI+  T + +FK
Sbjct  427 ALWKAQPDLPTASEAWILAGGAHHTVFSHALNLNDMRQFAEMHDIEITVIDNDTRLPAFK  486

Query  485 NELKWNEVFWRGR  497
           + L+WNEV++  R
Sbjct  487 DALRWNEVYYGFR  499
```

Appendix 3: Sequential alignment comparison of AAAI and GKAI

Sequence ID of GKAI: ref|YP_147757.1| **Length:** 497

From http://www.ncbi.nlm.nih.gov/pubmed/

Score	Expect	Method	Identities	Positives	Gaps
1001 bits(2589)	0.0	Compositional matrix adjust.	478/497(96%)	491/497(98%)	0/497(0%)

```
Query  1    MMLSLRPYEFWFVTGSQHLYGEEALKQVEEHSMMIVNELNQDSVFPFPLVFKSVVTTPEE  60
            MMLSLRPYEFWFVTGSQHLYGEEALKQVEEHS ++VNE N+DSVFPFP VFKSVVTTPEE
Sbjct  1    MMLSLRPYEFWFVTGSQHLYGEEALKQVEEHSRIMVNEWNRDSVFPFPFVFKSVVTTPEE  60

Query  61   IRRVCLEANASEQCAGVITWMHTFSPAKMWIGGLLELRKPLLHLHTQFNRDIPWDSIDMD  120
            IRRVCLEANASEQCAGV+TWMHTFSPAKMWIGGLLELRKPLLHLHTQFNRDIPWDSIDMD
Sbjct  61   IRRVCLEANASEQCAGVVTWMHTFSPAKMWIGGLLELRKPLLHLHTQFNRDIPWDSIDMD  120

Query  121  FMNLNQSAHGDREYGFIGARMGVARKVVVGHWEDPSVRERLAKWMRTAVAFAESRHLKVA  180
            FMNLNQSAHGDREYGFIGARMGVARKVVVGHWEDP VRERLAKWMRTAVAFAESR+LKVA
Sbjct  121  FMNLNQSAHGDREYGFIGARMGVARKVVVGHWEDPEVRERLAKWMRTAVAFAESRNLKVA  180

Query  181  RFGDNMREVAVTEGDKVGAQIQFGWSVNGYGVGDLVQYIRDVSEQKINELLEEYAELYDI  240
            RFGDNMREVAVTEGDKVGAQIQFGWSVNGYG+GDLVQYIRDVSEQK+NELL+EY ELYDI
Sbjct  181  RFGDNMREVAVTEGDKVGAQIQFGWSVNGYGIGDLVQYIRDVSEQKVNELLDEYEELYDI  240

Query  241  VPAGRQDGPVRESIREQARIELGLKAFLKDGNFAAFTTTFEDLHGMKQLPGLAVQRLMAE  300
            VPAGRQ+GPVRESIREQARIELGLKAFL+DGNF AFTTTFEDLHGMKQLPGLAVQRLMAE
Sbjct  241  VPAGRQEGPVRESIREQARIELGLKAFLQDGNFTAFTTTFEDLHGMKQLPGLAVQRLMAE  300

Query  301  GYGFGGEGDWKTAALVRLMKVMADGKGTSFMEDYTYHFEPGNEMILGAHMLEVCPTIAAT  360
            GYGFGGEGDWKTAALVRLMKVMADGKGTSFMEDYTYHFEPGNE+ILGAHMLEVCPTIAAT
Sbjct  301  GYGFGGEGDWKTAALVRLMKVMADGKGTSFMEDYTYHFEPGNELILGAHMLEVCPTIAAT  360

Query  361  RPRIEVHPLSIGGKEDPARLVFDGGEGAAVNASLIDLGHRFRLIVNEVDAVKPEHDMPKL  420
            RPR+EVHPLSIGGKEDPARLVFDGGEGAAVNASLIDLGHRFRLIVNEVDAVKPEHDMPKL
Sbjct  361  RPRVEVHPLSIGGKEDPARLVFDGGEGAAVNASLIDLGHRFRLIVNEVDAVKPEHDMPKL  420
```

```
Query  421  PVARILWKPRPSLRDSAEAWILAGGAHHTCFSFAVTTEQLQDFAEMAGIECVVINEHTSV  480
            PVARILWKPRPSLRDSAEAWILAGGAHHTCFSFAVTTEQLQDFAEMAGIECVVINEHTSV
Sbjct  421  PVARILWKPRPSLRDSAEAWILAGGAHHTCFSFAVTTEQLQDFAEMAGIECVVINEHTSV  480

Query  481  SSFKNELRWNEVFWRGR  497
            SSFKNEL+WNEVFWRGR
Sbjct  481  SSFKNELKWNEVFWRGR  497
```

ACKNOWLEDGEMENT

--- ☆ ---

This project would not have been possible without the support of many people.

First and foremost, I would like to express my sincere gratitude to *Prof. You Ho Jin, Doctor of Medicine*, who has guaranteed me to study in Chosun University, and *Prof. Lee Sung Haeng, Doctor of Medicine*, who has directly conducted me to complete this project.

I would like to thank *Mr. Choi Jin Myung*, he guided me all of the techniques involved in this project, and helped me to complete all the requirements in the thesis as well as in my graduation.

I would like to sincerely thank *Dr. Yun Cha Kyung*, *Dr. Ankita Shahi and her husband*, they taught me for a period and gave me the motivation of research.

I would like to give appreciative thanks to *my Venerable Teacher, Mrs. Lương Bảo Uyên, PhD*, she always gives me precious advices, and always be willing to support me at any time.

I would like to extend my warm thanks to *Mr. Trịnh Đức Anh* and his wife, *Mrs. Nguyễn Thị Huyên*, and to *Mr. Nguyễn Hồng Phương*, who are always willing to teach and help me since I came to Chosun University.

I would like to thank *all my friends* who are always beside me, my Korean, Indian, Nepalese and Vietnamese friends.

Finally, *my family*, and *my beloved*, are always my consolidated support.